OAK RIDGE NATIONAL LABORATORY LIBRARIES
3 4456 0548460 5

CENTRAL RESEARCH LIBRARY
DOCUMENT COLLECTION

OAK RIDGE NATIONAL LABORATORY

operated by

UNION CARBIDE CORPORATION

for the

U.S. ATOMIC ENERGY COMMISSION

ORNL-TM-26

COPY NO. - 90

DATE - October 1961

A SIMULATION OF THE EGCR STEAM GENERATOR

M. M. Yarosh and S. J. Ball

Abstract

An analog model of the EGCR steam generator was developed and operated on the ORNL analog computer as part of a program to simulate the operation and control of the EGCR reactor plant. Equilibrium operation and the transient response of the steam generator unit to system perturbations were studied. A simultaneous solution of the basic heat transfer equations representing the performance of the unit was obtained. The model was operated initially at steady-state conditions, and then perturbations were made to gas flow, gas inlet temperature, and steam throttle valve position. The response characteristics of the model during the transients were recorded. The steam generator gas outlet temperature showed a marked degree of insensitivity to changes in gas inlet temperature. The effect of gas flow changes on gas exit temperature was slightly more pronounced. The transient behavior of the unit was reasonable, and the model developed indicated satisfactory operation within the design range of 20 to 100% of full power.

CENTRAL RESEARCH LIBRARY
DOCUMENT COLLECTION
LIBRARY LOAN COPY
DO NOT TRANSFER TO ANOTHER PERSON
If you wish someone else to see this document, send in name with document and the library will arrange a loan.

NOTICE

This document contains information of a preliminary nature and was prepared primarily for internal use at the Oak Ridge National Laboratory. It is subject to revision or correction and therefore does not represent a final report. The information is not to be abstracted, reprinted or otherwise given public dissemination without the approval of the ORNL patent branch, Legal and Information Control Department.

LEGAL NOTICE

This report was prepared as an account of Government sponsored work. Neither the United States, nor the Commission, nor any person acting on behalf of the Commission:

A. Makes any warranty or representation, expressed or implied, with respect to the accuracy, completeness, or usefulness of the information contained in this report, or that the use of any information, apparatus, method, or process disclosed in this report may not infringe privately owned rights; or

B. Assumes any liabilities with respect to the use of, or for damages resulting from the use of any information, apparatus, method, or process disclosed in this report.

As used in the above, "person acting on behalf of the Commission" includes any employee or contractor of the Commission, or employee of such contractor, to the extent that such employee or contractor of the Commission, or employee of such contractor prepares, disseminates, or provides access to, any information pursuant to his employment or contract with the Commission, or his employment with such contractor.

cy 90

To: ORNL-TM-26 Listed Distribution

Subject: Errata sheets for ORNL-TM-26

Please replace pages 3, 41, 42, and 43 of subject memorandum with the attached pages.

Table of Contents

Section			Page
I		Introduction	4
II		EGCR Steam Generator Description	5
III		Heat Transfer	9
	A	Superheater Section	9
	B	Evaporator Section	13
	C	Economizer Calculations	14
IV		Description of the Analog Computer Model	15
	A	Superheater Section	15
	B	Evaporator Section	19
	C	Economizer Section	21
	D	Turbine, Throttle Valve, and Pressure Control System	23
V		Operation and Results	24
	A	Equilibrium Operating Conditions	24
	B	Turbine under Pressure Regulator Control	24
	C	Turbine Control Valve Position Constant	47
VI		Conclusions and Recommendations	52
APPENDIX		Summary of Equations Used in Analog Model	55

OAK RIDGE NATIONAL LABORATORY LIBRARIES

3 4456 0548460 5

I. Introduction

The design of a satisfactory control system for the EGCR requires a comprehensive understanding of the response of the plant to perturbations imposed on the reactor and steam plant complex. In order to further this understanding, the entire reactor plant was simulated on an electronic analog computer. As part of this program, an analog model of the EGCR steam generator was developed and operated on the ORNL analog computer.

The development of such a model requires a satisfactory mathematical description of the heat transfer performance of the unit. Transient conditions existing after imposing perturbations to an equilibrium condition are determined by the simultaneous solution of these equations during the transient period.

The present study investigated steam generator response to changes in gas inlet temperature, gas flow, and steam flow with the unit always operating within the design range of 20 to 100% of full power. Some investigation, however, was also made of the effect of a reactor scram or a loss of power on the steam generator performance.

A series of graphs are included which represent the transient response of the steam generator to the input perturbations. Also shown are equilibrium operating temperatures and flows for the helium and steam at 20 to 100% power levels.

II. EGCR Steam Generator Description

Figure 1 is a drawing of the EGCR steam generator. The unit is basically a single-pass gas crossflow heat exchanger. Gas enters the pressure vessel at the midheight of the tube bundle through the 24-in. entrance nozzle. The gas passes into the distribution shroud, impinges on the tube entrance baffle plate, is distributed vertically along the length of the tube bundle, and then passes across the tube bundle. The discharge gas flows around the outside of the bundle shroud and out the discharge nozzle.

Feedwater enters the economizer section of the steam generator in the bottom floating drum and makes five passes across the gas path before discharging into the steam drum. The feedwater returns to the floating drum through the central downcomer pipe and flows up the evaporator tubes to the steam drum. Saturated steam is discharged from the steam drum through an external pipe to the superheater entrance in the bottom floating head. The steam is superheated in four passes across the gas path and is discharged from the bottom floating head. Section BB of Fig. 1 shows the arrangement of economizer, evaporator, and superheater tubes within the bundle shroud. Figure 2 is an isometric view of the unit. Table I gives additional data on the steam generator.

The steam generator is one of two identical units that together provide the necessary cooling capacity for the reactor. Each generator has a rated capacity of 147×10^6 Btu/hr (43 Mw), and their steam outputs are combined to drive a turbine-generator unit producing 29 Mwe. Throughout the study it was assumed that there was no interaction between the two steam generators.

UNCLASSIFIED
ORNL-LR-DWG-60899

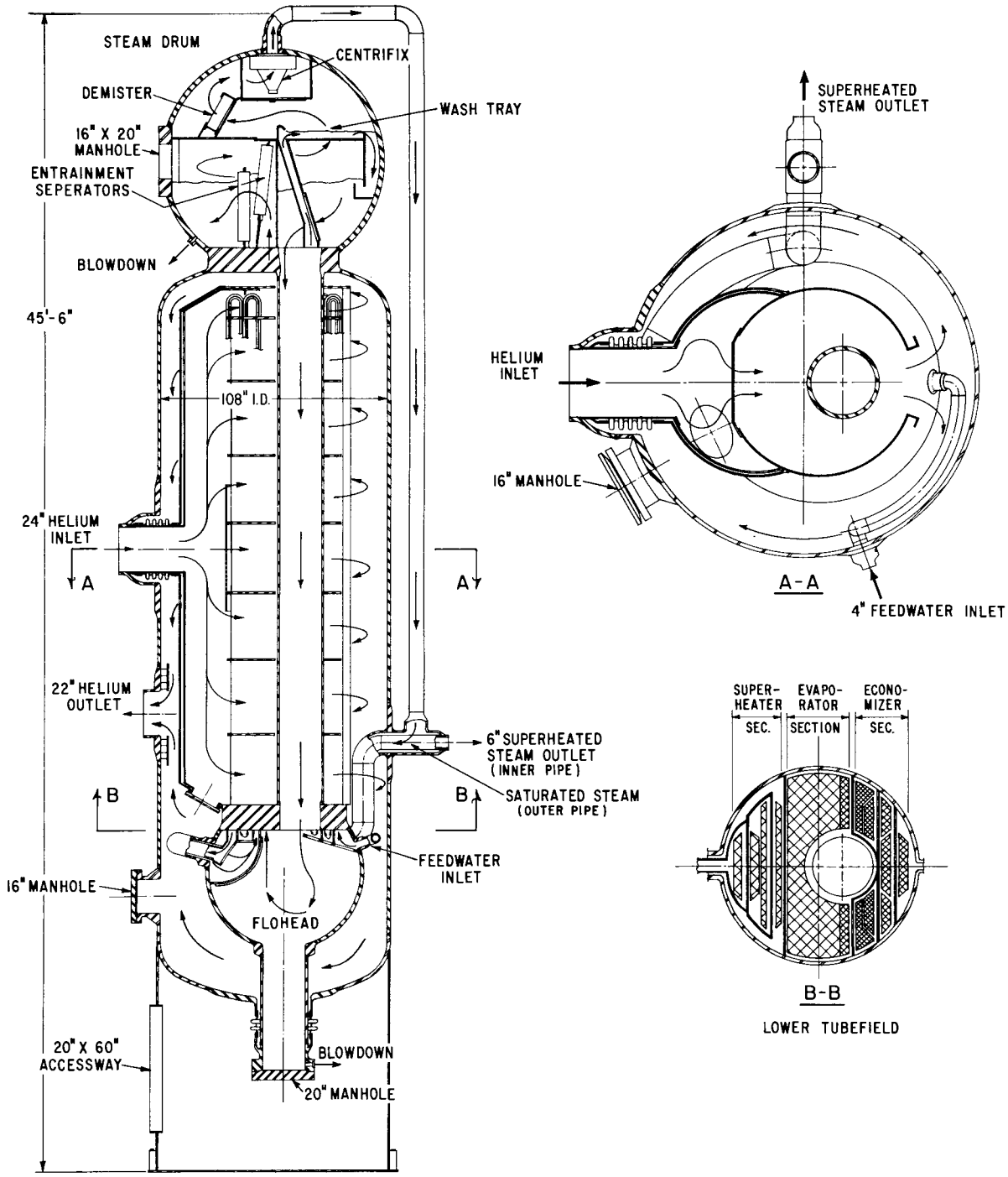

EGCR STEAM GENERATOR

ARROWS INDICATE FLOW DIRECTION

FIGURE 1.

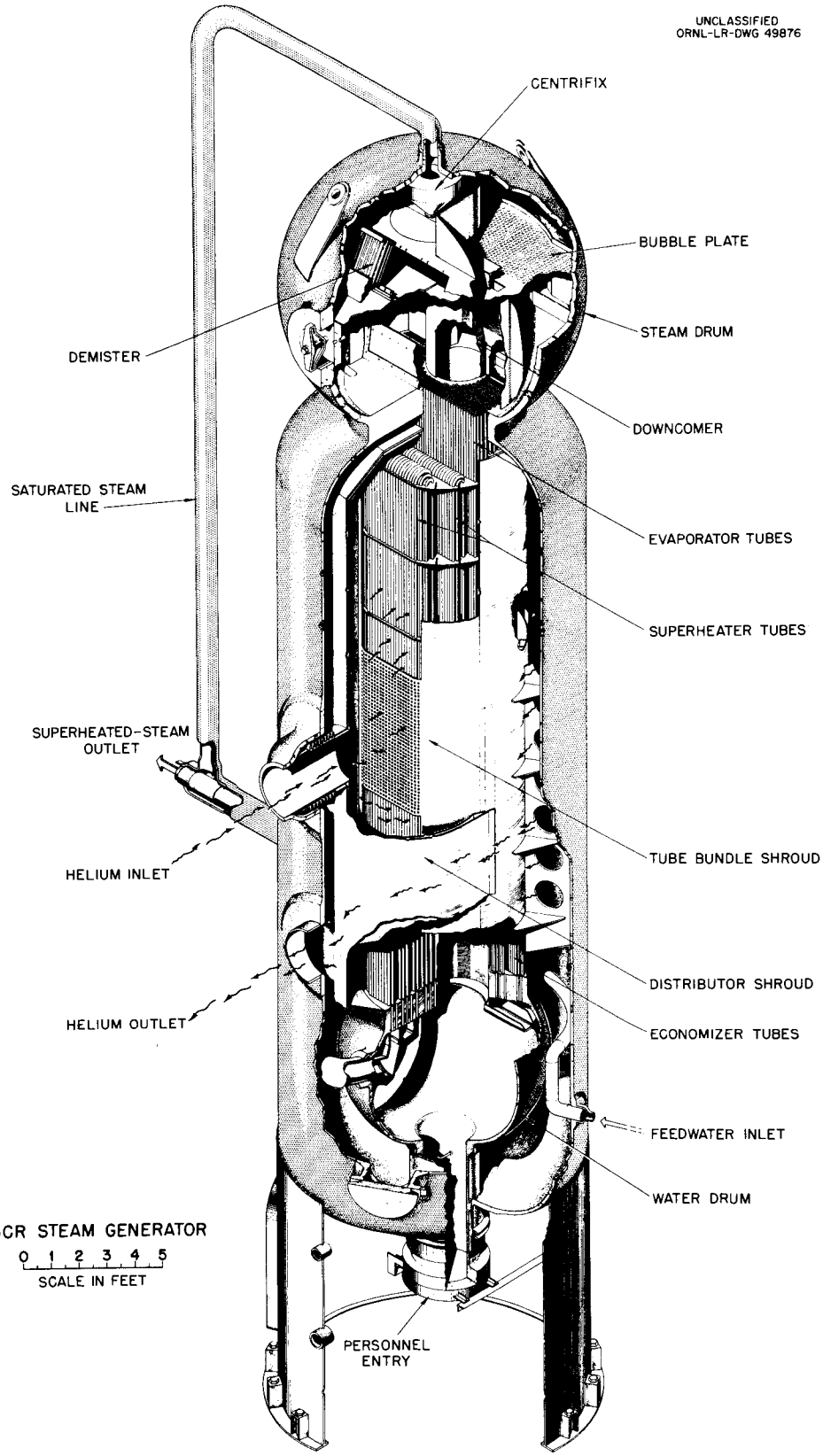
UNCLASSIFIED
ORNL-LR-DWG 49876
CENTRIFIX
BUBBLE PLATE
STEAM DRUM
DEMISTER
DOWNCOMER
SATURATED STEAM LINE
EVAPORATOR TUBES
SUPERHEATER TUBES
SUPERHEATED-STEAM OUTLET
TUBE BUNDLE SHROUD
HELIUM INLET
DISTRIBUTOR SHROUD
HELIUM OUTLET
ECONOMIZER TUBES
FEEDWATER INLET
WATER DRUM
EGCR STEAM GENERATOR
0 1 2 3 4 5
SCALE IN FEET
PERSONNEL ENTRY

TABLE I

EGCR Steam Generator Design Data

	Economizer		Evaporator I	Evaporator II	Evaporator III	Superheater
Tube outside diameter, in.	3/4	3/4	3/4	1	1	1
Tube inside diameter, in.	0.495	0.495	0.495	0.709	0.834	0.782
Tube length, ft (40-ft tubes are U-tubes)	40.08	20.25	20.25	20.25	20.25	40.08
External surface type	finned	finned	finned	finned	bare	bare
Tube pitch, in. (60-deg equilateral spacing)	15/16	15/16	15/16	1 1/4	1 1/4	1 1/4
Area ratio, outside area/inside area	3.86	3.86	3.86	3.66	1.23	1.31
Outside area, ft^2	3750	1350	1000	4020	1380	1460
Number of tubes	190	134	98	294	261	139
Water-side passes in section	4	1	1	1	1	4
Number of tube rows	17*	17*	3	10	6	10
Tube material	carbon steel	carbon steel	carbon steel	carbon steel	carbon steel	1 1/4 Cr 1/2 Mo

*Straight and U-tubes intermixed over four-row interval.

III. Heat Transfer

Calculation of the heat transfer capacity of the EGCR steam generator is complicated by the following factors:

1) The free-flow area for gas varies significantly across the tube bundle so that the gas mass velocity and hence gas-side heat transfer coefficient is a function of the position within the steam generator.

2) The heat transfer coefficient also varies slightly with gas temperature within the steam generator.

The calculation of the over-all heat transfer coefficient for each section of the steam generator utilized certain approximations to simplify the simulation. In computing the capacities of the individual sections of the EGCR steam generator, corrections to the countercurrent log mean temperature differences for the existing flow geometry were not made. Values of log mean temperature used in the simulation are estimated to be approximately 2 to 5% above actual values.[1] The approximation in driving force temperature, however, has little effect on the transient analysis results, and a marked reduction in complexity of the simulation is effected by the assumptions made.

A. Superheater Section

The gas mass velocity across the superheater was computed for several positions in the superheater, and the effect on gas velocity of the variation in free-flow area was approximated by linearizing the changing flow area across the 10 tube rows of the superheater. Figure 3 shows the variation of the gas-side coefficient as a function of gas free-flow area for the superheater section assuming the linear change in flow area. The positions of row 1 (at the gas entrance) and row 10 are shown on the graph. The gas-

ORNL-LR-Dwg. 64225
Unclassified

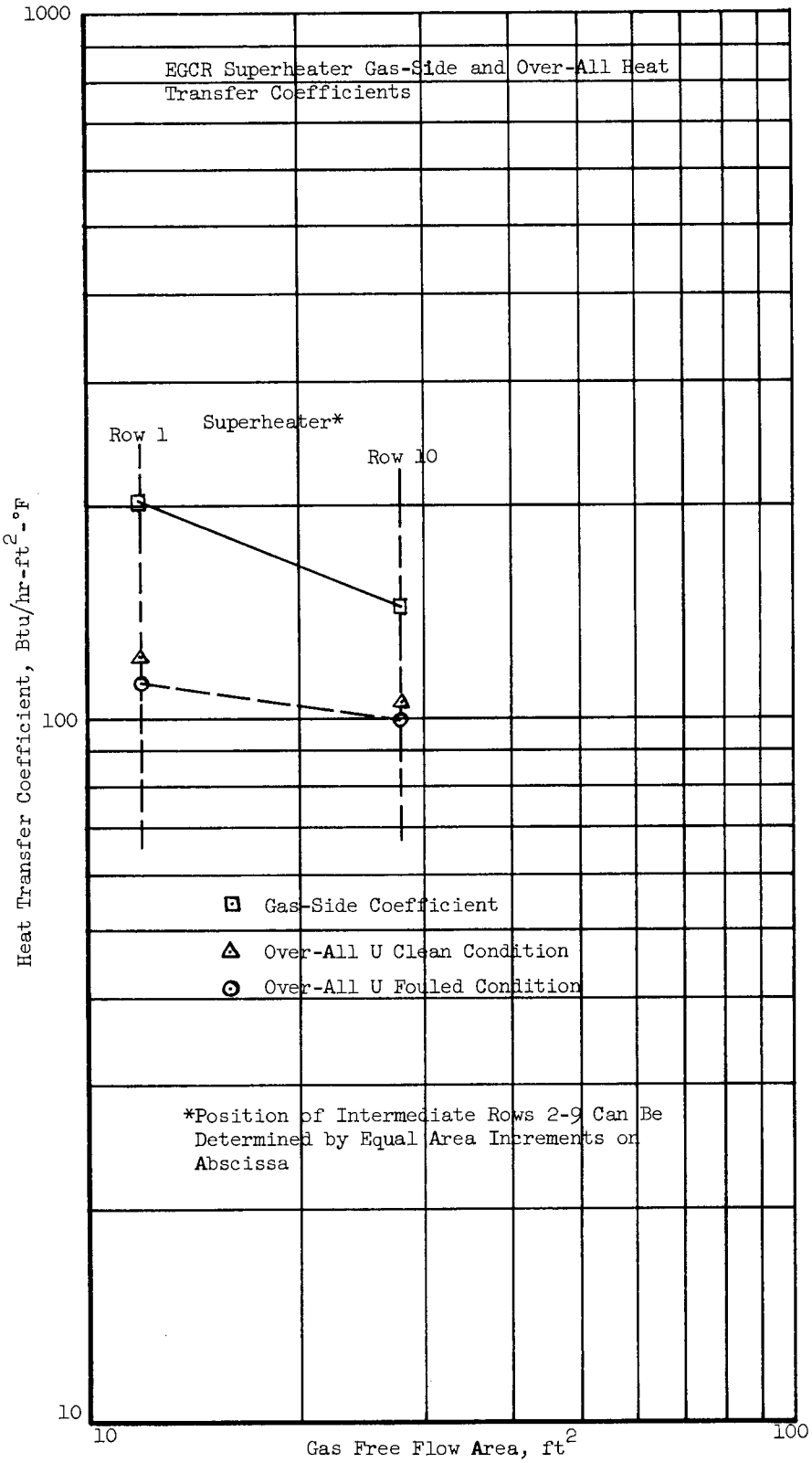

Fig. 3

side heat transfer coefficient for crossflow with bare tubes was obtained using the Colburn correlation for flow across banks of staggered tubes.[2]

$$\frac{h\,D_o}{k_f} = 0.33 \left[\frac{C_p\,\mu}{k}\right]^{1/3} \left[\frac{D_o\,G_{max}}{\mu_f}\right]^{0.61} \tag{1}$$

Steam-side coefficients were computed using the correlation of McAdams, Kennel, and Addoms.[3]

$$Nu = 0.0214 \left(1 + \frac{2.3}{L/D}\right) (Re)_f^{\,0.8}\,(Pr)_f^{\,1/3} \tag{2}$$

which for the EGCR steam generator may be reduced to:

$$h = \frac{0.0214\,G^{0.8}}{d_i^{\,0.2}} \left\{\frac{C_p\,\mu^{0.2}}{(Pr)^{2/3}}\right\} \tag{3}$$

The corresponding gas-side and steam-side coefficients for each row could have been obtained by a process of iterative calculations, but there was not available electronic equipment to permit such a detailed simulation. Corresponding gas-side and steam-side coefficients for rows 1 and 10 of the superheater were computed, and from these values the over-all U values for these rows were calculated. The over-all heat transfer coefficient was then assumed to vary with constant exponent as shown on Fig. 3. The variation of steam-side coefficient with steam temperature as computed from Eq. (3) is shown on Fig. 4. The large variation is a result of the radical change in thermal properties of the steam between saturated and superheated conditions.

Also shown in Fig. 4 is the percentage of superheater load (for 903°F steam) as a function of steam temperature. As seen on the graph, the high specific heat of steam near saturation conditions shifts the heat load towards the low-temperature portion of the

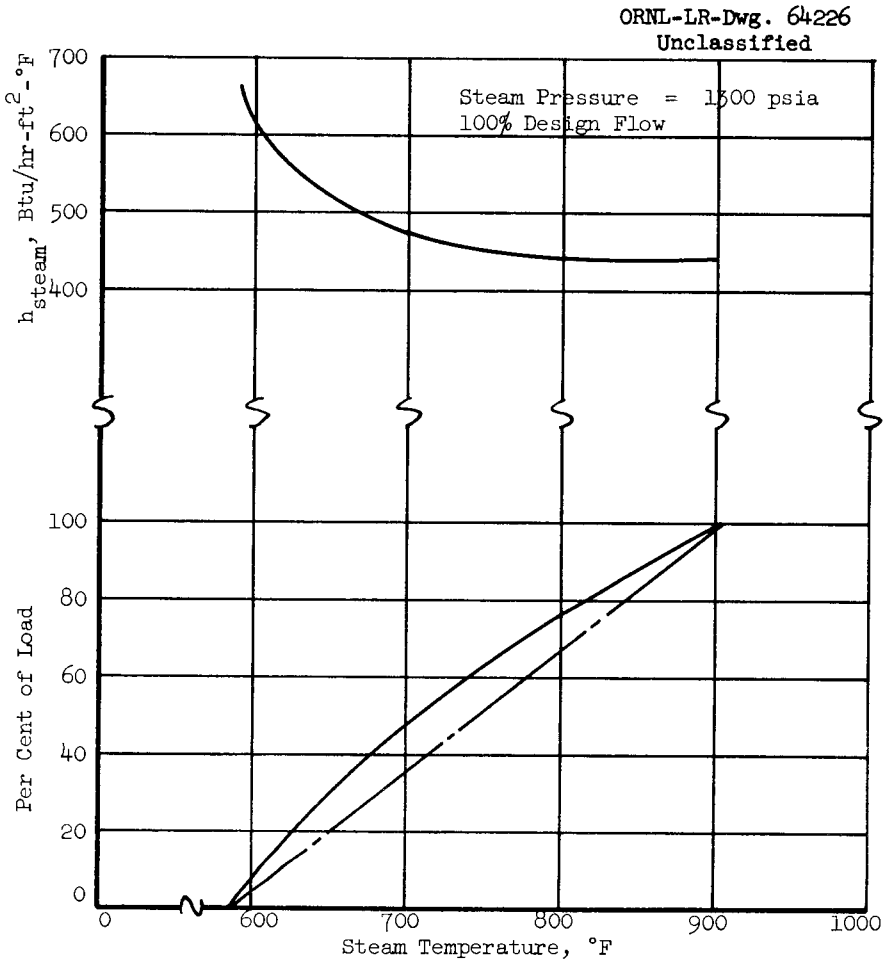

Fig. 4. Superheater Steam Heat Transfer Coefficient and Superheater Load Distribution as Functions of Steam Temperature

superheater. The relative load of the superheater at any temperature is indicated by the ratio of the slope of the solid curve at that temperature to the constant slope of the dashed curve.

B. Evaporator Section

As shown in Table I, the EGCR evaporator consists of three sections of tubes. The variation in gas velocity across the evaporator was approximated by computing an average mass velocity across each section. The temperature driving force was computed between gas temperature and saturation temperature corresponding to EGCR saturation pressure. The effect of fin efficiency was neglected, since for the low fin design and the design mass velocities for the EGCR, fin efficiencies will exceed 95% in all cases.[4] It was recognized that the simulated response of the system to perturbation would not be greatly affected by the approximations to the temperature driving force and the fin efficiency. However, the equilibrium levels at which the simulation showed the reactor system would operate would be affected to the extent of the influence of the approximation on steam generator capacity.

For purposes of the simulation a boiling coefficient of 3000 Btu/hr-ft^2-°F was selected, and this value was used throughout the simulation. Gas-side heat transfer coefficients for flow across banks of staggered finned tubes were obtained using the following equation derived from data obtained in Refs. 5 and 6:

$$j = 1.38\ Re^{-0.39}$$

where the equivalent diameter for the Reynolds number is defined as:

$$D_e = \frac{Nd_f}{12}\left(\frac{S}{d_t}\right)^2$$

The temperature driving force was computed for a heat exchanger with a constant sink temperature.

C. Economizer Calculations

The correlation for gas-side heat transfer coefficients was that used in the previous sections. Water-side coefficients were computed using the Dittus-Boelter correlation.

The location of the economizer section with respect to the downcomer and within the changing shroud area (see Fig. 1) produces gas-side mass velocities which decrease from maximum to minimum by approximately 40%. An average gas mass velocity across the economizer was selected for computing economizer capacity.

Implicit in the equations used for determining the heat transfer capacity of the steam generator was the assumption of uniform gas flow across the steam entrance face of the tube bundle. In addition, it was assumed that the gas mass velocity is uniform at any cross section as the gas proceeds across the tube bundle.

In the analysis of the steam generator performance during transient operating conditions equations were written for each section of the steam generator including terms representing the mass of metal and the capacity of the tube-side fluid. This is explained in more detail in Section IV.

A constant fouling factor of 0.0005 (Btu/hr-ft^2-°F) was used throughout.

IV. Description of the Analog Computer Model

The simulation of the EGCR steam generator involves the simultaneous solution of many nonlinear, partial differential equations and of several equations requiring iterative solution techniques. Since each of the three regions of the steam generator is in itself a somewhat complex system, a separate study employing fine breakdown and including nonlinear effects was made, when required, on a given region. The results of these investigations then made it possible to simplify the models without seriously affecting their performance. The simplified models, when interconnected, could then be assumed to give a fairly accurate representation of the behavior of the entire unit.

The analog model was set up to accommodate continuously varying gas, steam, and water flow rates and temperatures, and variable steam pressure. The useful operating range was to be nominally 20 to 100% of full power which corresponds to the range of the reactor's automatic control system.

A block diagram of the simulation is shown in Fig. 5 and is explained in detail in the following sections.

The appendix contains a description of the equations used in the analog model. Figures A-9 through A-14 in the appendix show the nonlinear relationships between the various steam generator parameters and the corresponding approximations used in the analog model. Figure A-15 is the computer circuit schematic used.

A. Superheater Section

The superheater was assumed to be a counterflow heat exchanger with both steam- and gas-side properties as continuous functions of their respective flow rates. A three-lump breakdown (in the direction of flow) was required for an accurate solution of the steam-side

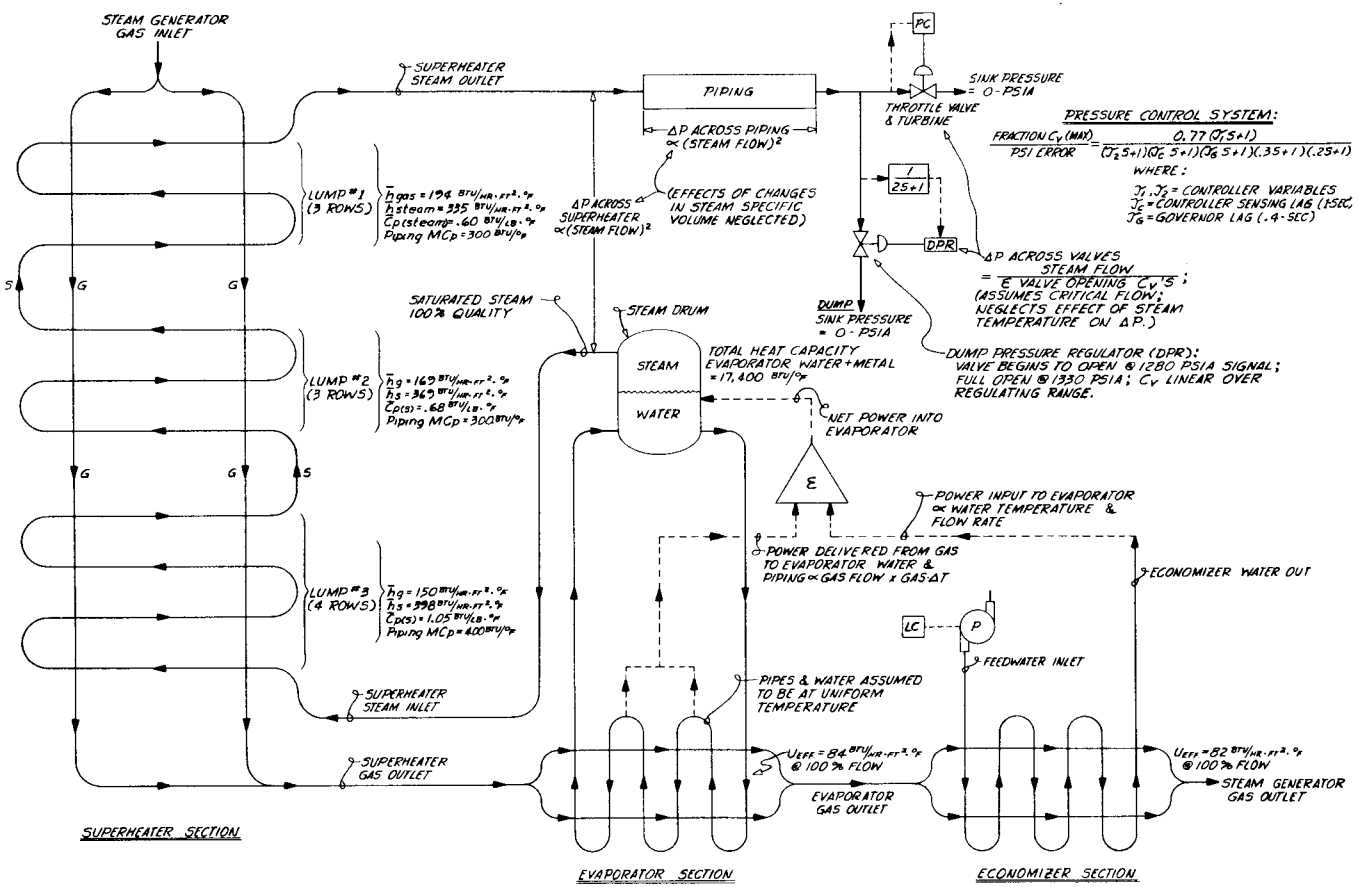

NOTE:

HEAT TRANSFER COEFFICIENT (h) VALUES SHOWN ARE FOR 100% RATED FLOW CONDITIONS:
HELIUM FLOW RATE (wg) = 215,000 #/hr (59.7 LB/sec)
STEAM FLOW RATE (ws) = 127,700 #/hr (35.5 LB/sec)

EGCR STEAM GENERATOR

FIG. 5. BLOCK DIAGRAM OF SIMULATION FOR CONTROL STUDY

transients.* Mean values of the steam-side heat transfer coefficient ($\bar{h}_s$) and the steam specific heat ($\bar{C}_{p(s)}$) in each lump were determined at full load by trial and error methods using the computer model. The iterative procedure was necessary because of the strong temperature dependence of $\bar{h}_s$ and $\bar{C}_{p(s)}$. Once these values were established, however, they were assumed to be independent of temperature changes.

An analog model using a five-lump breakdown with values of $\bar{h}_s$ and $\bar{C}_{p(s)}$ as continuous functions of temperature was constructed so that the adequacy of the three-lump model could be judged. Figure 6 shows the response to step changes in gas inlet temperature for three initial gas temperatures. Note that the steam-side temperature dependence becomes noticeable when the gas inlet temperature drops below 800°F. Figure 6 also shows an instantaneous drop in superheater gas outlet temperature for a step inlet change. This is because the transport lag time of the gas was neglected. This approximation contributes negligible error in this case since the transport lag time is very small compared to the thermal time constants. As noted on the figure the use of the three-lump breakdown with constant steam properties gave results almost identical to those obtained using the five-lump breakdown including temperature-dependent properties.

The gas-side free-flow area varies significantly across the superheater section, and this is largely responsible for the change in gas-side coefficient from lump to lump.

The dependence of steam properties with pressure is not significant for small changes in pressure and was neglected in both models.

---

*An "x-lump" breakdown means that the partial differential equations describing the system were reduced to "x" sets of total differential equations using standard finite difference techniques.

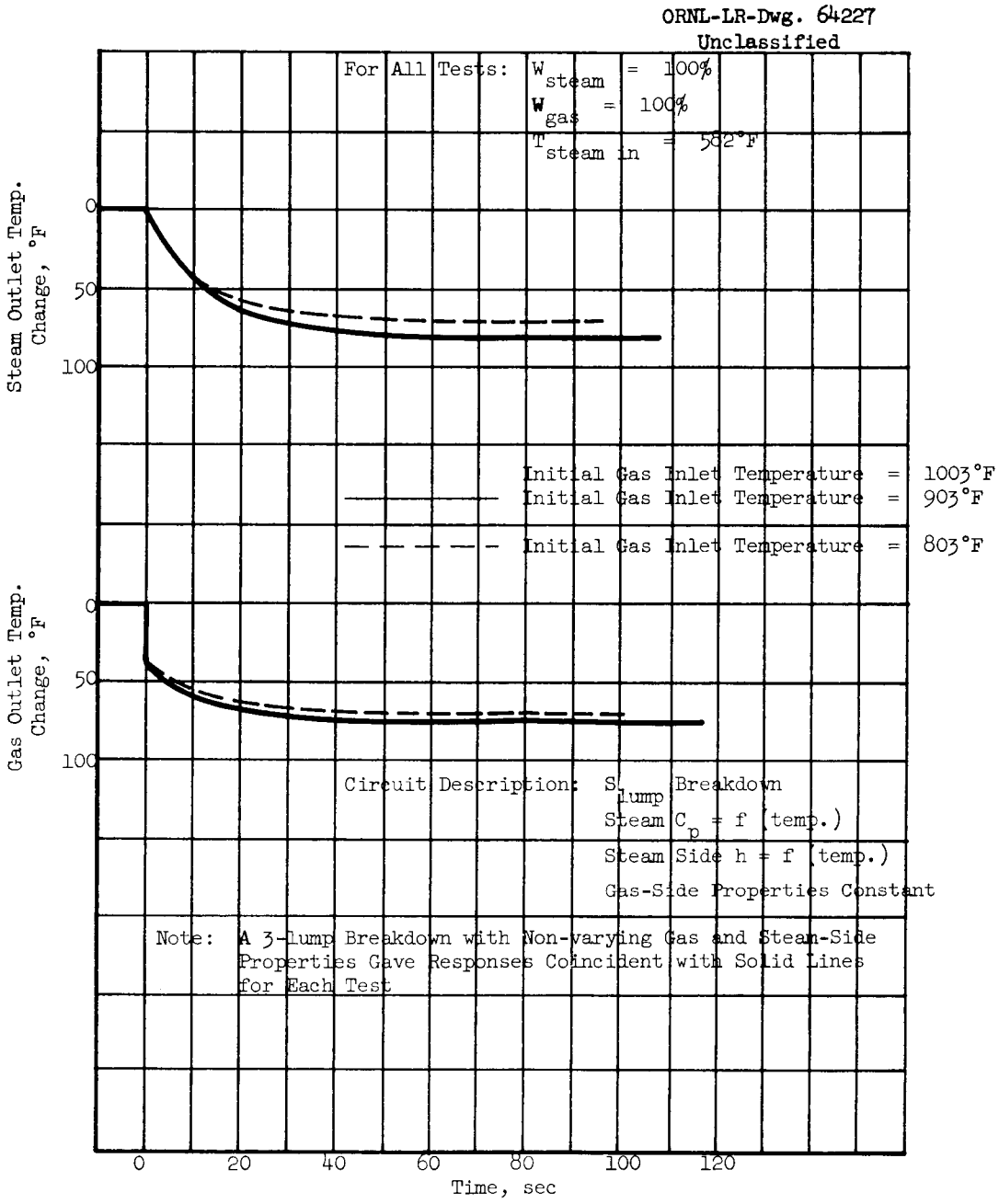

Fig. 6. Responses to 100°F Step Decreases in Gas Inlet Temperature Showing Effects of Variations in Starting Point Temperatures

B. Evaporator Section

It was assumed that the temperature of the water in the evaporator was uniform (saturation temperature), and because the combination of boiling and fouling heat transfer coefficients is much larger than the gas-side coefficient, the water and tubes were assumed to form an essentially constant temperature sink for the gas. For a heat exchanger with a constant sink temperature, it is convenient to express the heat transfer capacity as a function in the form:

$$\left(\frac{T_{gas\ in} - T_{gas\ out}}{T_{gas\ in} - T_{sink}}\right) \qquad \%$$

a function which varies only with gas flow rate. Knowing the gas inlet temperature, the sink temperature, and the gas flow rate, one can then determine the evaporator gas outlet temperature. The instantaneous power delivered from the gas to the tube is the product of gas flow rate, gas temperature drop, and specific heat.

Because the combination of boiling scale and tube resistances, although small, was actually not negligible compared to the gas-side resistance; a fine-structure analog model was subsequently constructed in order to evaluate the original approximations. The results showed that the gas outlet temperature and power are not strictly instantaneous functions of inlet temperature and flow but are lagged by a function which closely approximates a first-order lag with a 3-sec time constant. This lag was not included in the model used for this report.

The calculation of the pressure in the evaporator was complicated by the fact that the pressure is a function of the relationships between the rates of heat transfer from the gas, the temperature and flow rate of the water entering the evaporator from the economizer, and the steam flow rate. The steam flow rate is, in turn, a function of the evaporator pressure, the pressure drop

across the superheater and the steam piping, and the condition of the turbine and throttling and dump valves. The basic equality:

$$P_{evaporator} = \Delta P_{superheater} + \Delta P_{piping} + \Delta P_{valve\ and\ turbine} + P_{sink}$$

was solved continuously by a computing process which determined the value of steam flow rate which satisfied the equation. The pressure drop across the superheater and piping was assumed to be a function of the square of the steam flow rate, and the drop across the turbine and throttling valve was calculated (assuming critical flow) from:

$$\Delta P_{valve\ \&\ turbine} \propto \frac{\text{steam flow rate}}{\text{effective valve } C_v}$$

Thus the pressure drop characteristics of the valve and turbine were approximated by one valve with linear trim.

Evaporator pressure was computed from the density of steam in the evaporator. This value was obtained by assuming a constant steam volume in the evaporator and determining the mass of steam within. This mass of steam was in turn a time integral function of the difference in the steam generation rate as computed from the heat transfer through the evaporator and the steam effluent rate as computed from the pressure drop equations.

A condition of nonequilibrium exists when the temperature corresponding to the pressure as computed above is different from the actual bulk temperature in the evaporator. Since both superheated and supercooled water are unstable, such temperature differences would cause steam to be either flashed off or condensed in order to restore equilibrium conditions. In the computer model, an unstable condition caused a variation in the total steam flow rate according to:

$$\Delta W_{steam} = K\,(T_{water} - T_{saturation})$$

where K is a large number. A heat balance was maintained by changing the heat content of the evaporator water and metal by an amount equal to the integrated heat content of ΔW_{steam}.

The drum level controller, which controls from a combined level and steam-to-water flow ratio signal, was assumed to make the feedwater mass flow rate always equal to the steam mass flow rate. Since the response of the level controller would generally be fast compared to changes in steam flow rate, this assumption would produce negligible error. Also, since the steam and water flow rates were assumed equal, the net rate of sensible heat input to the evaporator could be computed from the product of feedwater flow and the difference between the temperature of the water entering the evaporator and saturation temperature.

C. Economizer Section

The usual method of heat exchanger simulation involves one or more sets of computations for heat transfer between one fluid and the pipe, heat storage in the pipe, transfer between the pipe and the other fluid, and fluid transport lags (where required). In the evaporator, however, the over-all thermal dynamics are dominated by the effects of the transport lag time of the water, the water transport time being 28 sec at 100% flow, while the approximate time constant for heat transfer through the pipe is 7 sec. Thus the use of the conventional simulation techniques would require a prohibitively large amount of computing equipment.

An analog model was developed which uses a power balance relationship in which the power delivered from the gas to the economizer water and piping is proportional to the product of gas flow rate and gas temperature change across the economizer. The effects of gas inlet temperature and flow rate changes on the mean water (and pipe) temperature take place as a first-order lag approximation to a ramp function with a 28-sec duration (at 100% flow), as

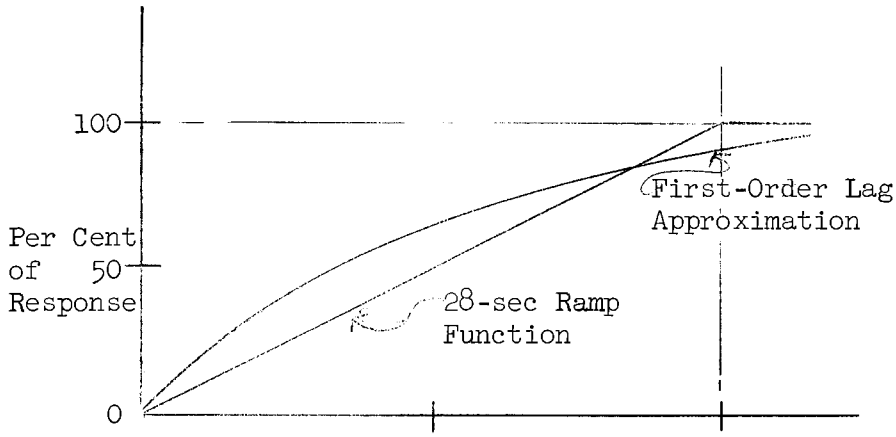

Fig. 7. Comparison of 28-sec Ramp Function and First-Order Lag Approximation

shown in Fig. 7. The effects of changes in feedwater inlet temperature and flow rate on the mean temperature of the water and pipes are also functions of the ramp approximation.

The effective over-all heat transfer coefficient (U) in the economizer is a function of both the gas- and water-side coefficients. Due to the nature of the simulation techniques used, it was necessary to make linearized approximations of the actual heat transfer mechanism. A two-lump heat transfer computer circuit on the gas side was adjusted to give exact effective log mean ΔT transfer for 100% and 20% full-load conditions, assuming equal gas and water flow rates (percentage wise). In between 100% and 20%, the effective U was assumed to vary as the gas-side coefficient, which is dominant. During transient gas flow conditions and for large changes in steam generator inlet gas temperature, however, the gas and water flow rates are not equivalent, and the effective U value varies significantly from the computation which assumes balanced flow rates. Calculations and test runs covering a wide range of input changes (150°F changes in inlet temperature and 20% step

changes in gas flow) show that the maximum departure of gas and water flow rates is about 20%. A computer circuit to account for this unbalance was used which gives a linear approximation to the actual U values for up to a 20% departure.

As before, the fin efficiency variation and the gas transit time in the economizer were neglected.

D. Turbine, Throttle Valve, and Pressure Control System

As noted previously, the turbine and throttle valve were simulated by assuming that their combined action could be characterized by one valve whose opening (C_v) was proportional to the output of the positioning device. Because of the large pressure drop across the "valve" and the low sink pressure, the flow was assumed to be in the "critical" range. The effects of steam temperature changes on the flow are small and were neglected.

The pressure regulator control system attempts to maintain a constant pressure upstream of the throttle valve by varying the valve opening. The characteristics of the control system were taken from the manufacturer's data and are shown on the block diagram (Fig. 5). It was found that the effects of the controller and actuator lags on the performance of the unit were negligible and were omitted from the simulation. The automatic reset feature of the controller was included, however.

V. Operation and Results

The salient results of the various input perturbations imposed on the steam generator appear in Figs. 11 to 23. Table II lists the equilibrium and transient runs investigated and the important perturbations imposed during each run.

A. Equilibrium Operating Conditions

Utilizing the heat transfer coefficients derived from the equations given in Section III, equilibrium operating conditions for the steam generator were determined. Figure 8 shows the equilibrium operating conditions for a constant steam temperature of 903°F leaving the superheater as a function of helium flow rate. Figure 9 similarly shows operating conditions for a constant gas temperature of 1043°F entering the steam generator. In each case the feedwater inlet temperature was varied in accordance with Fig. 10. The conditions were repeated using a modified gas-side coefficient, and the results are also shown on the graphs. Because of the assumptions made about the log mean temperature difference, the fin efficiency, and the fouling factor, the unit capacity shown by the solid lines in Figs. 8 and 9 may be somewhat high. A modified coefficient representing a reduction in the gas-side coefficient of approximately 10% more nearly represents probable equilibrium conditions. This modification was examined in order to confirm that the transient response of the system would be insensitive to small errors in the computer heat transfer capacity of the system.

B. Turbine under Pressure Regulator Control

1. Changes in Gas Flow

The characteristic effects of a large change in gas flow through the steam generator system are shown in Fig. 11, Run D-1. A step

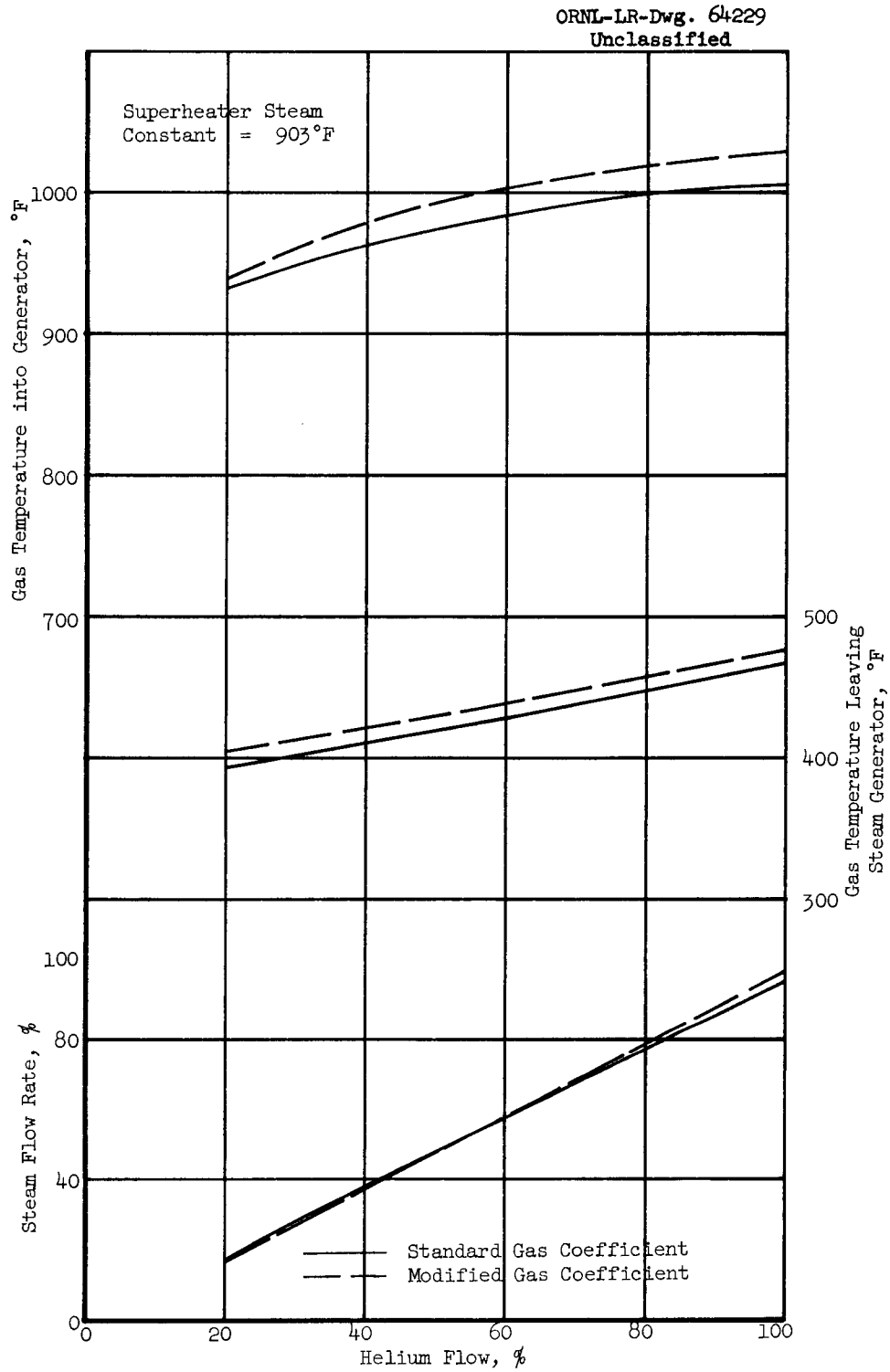
ORNL-LR-Dwg. 64229
Unclassified
Superheater Steam
Constant = 903°F
Gas Temperature into Generator, °F
1000
900
800
700
500
400
300
Gas Temperature Leaving
Steam Generator, °F
100
80
40
0
Steam Flow Rate, %
Standard Gas Coefficient
Modified Gas Coefficient
0
20
40
60
80
100
Helium Flow, %

Fig. 8

ORNL-LR-Dwg. 64230
Unclassified

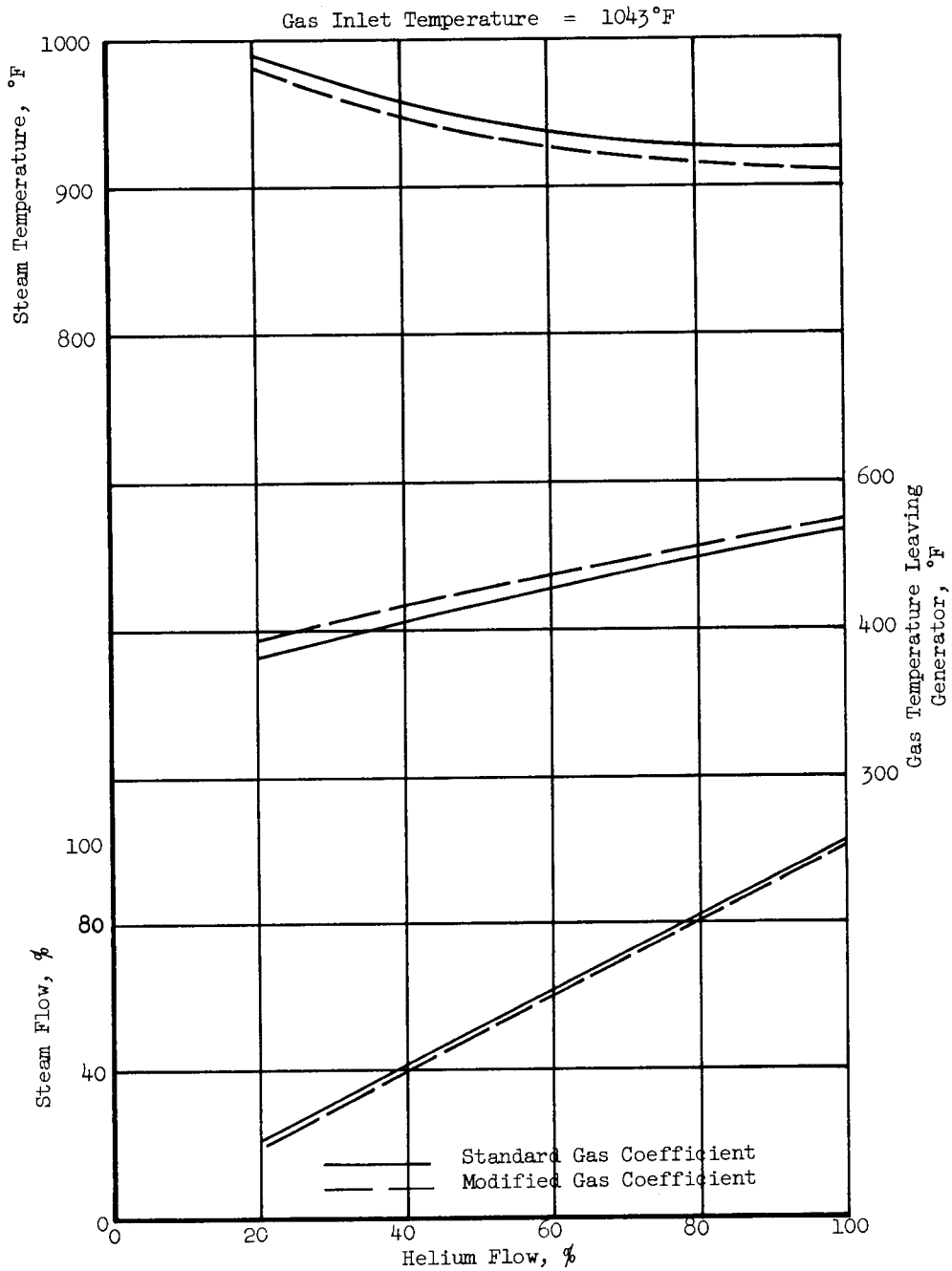

Fig. 9

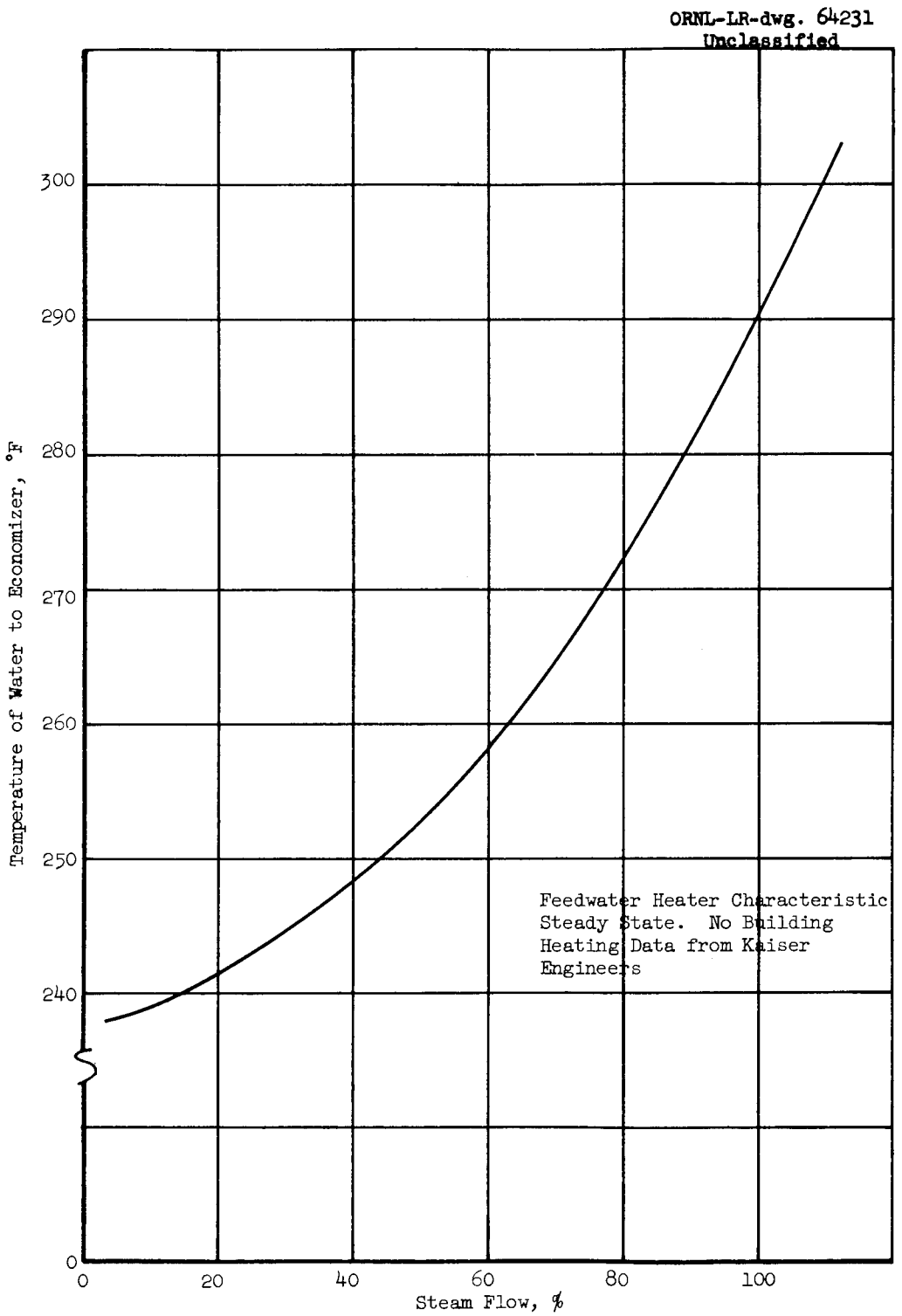
ORNL-LR-dwg. 64231
Unclassified
Temperature of Water to Economizer, °F
300
290
280
270
260
250
240
0
0
20
40
60
80
100
Steam Flow, %
Feedwater Heater Characteristic
Steady State. No Building
Heating Data from Kaiser
Engineers

Fig. 10

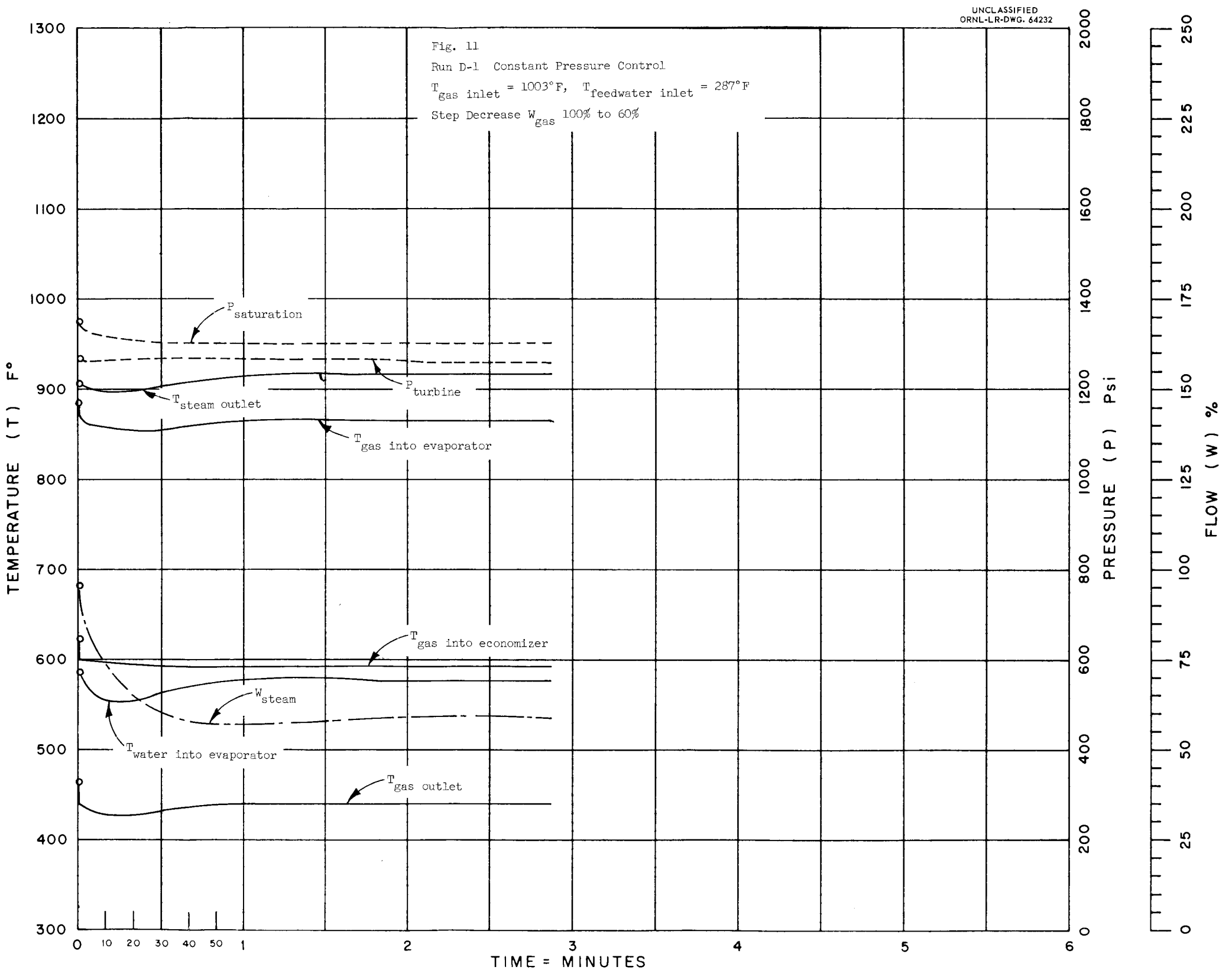
UNCLASSIFIED
ORNL-LR-DWG. 64232
Fig. 11
Run D-1 Constant Pressure Control
$T_{gas\ inlet}$ = 1003°F, $T_{feedwater\ inlet}$ = 287°F
Step Decrease W_{gas} 100% to 60%
$P_{saturation}$
$P_{turbine}$
$T_{steam\ outlet}$
$T_{gas\ into\ evaporator}$
$T_{gas\ into\ economizer}$
W_{steam}
$T_{water\ into\ evaporator}$
$T_{gas\ outlet}$
TEMPERATURE (T) F°
PRESSURE (P) Psi
FLOW (W) %
TIME = MINUTES
1300
1200
1100
1000
900
800
700
600
500
400
300
2000
1800
1600
1400
1200
1000
800
600
400
200
0
250
225
200
175
150
125
100
75
50
25
0
0
10
20
30
40
50
1
2
3
4
5
6

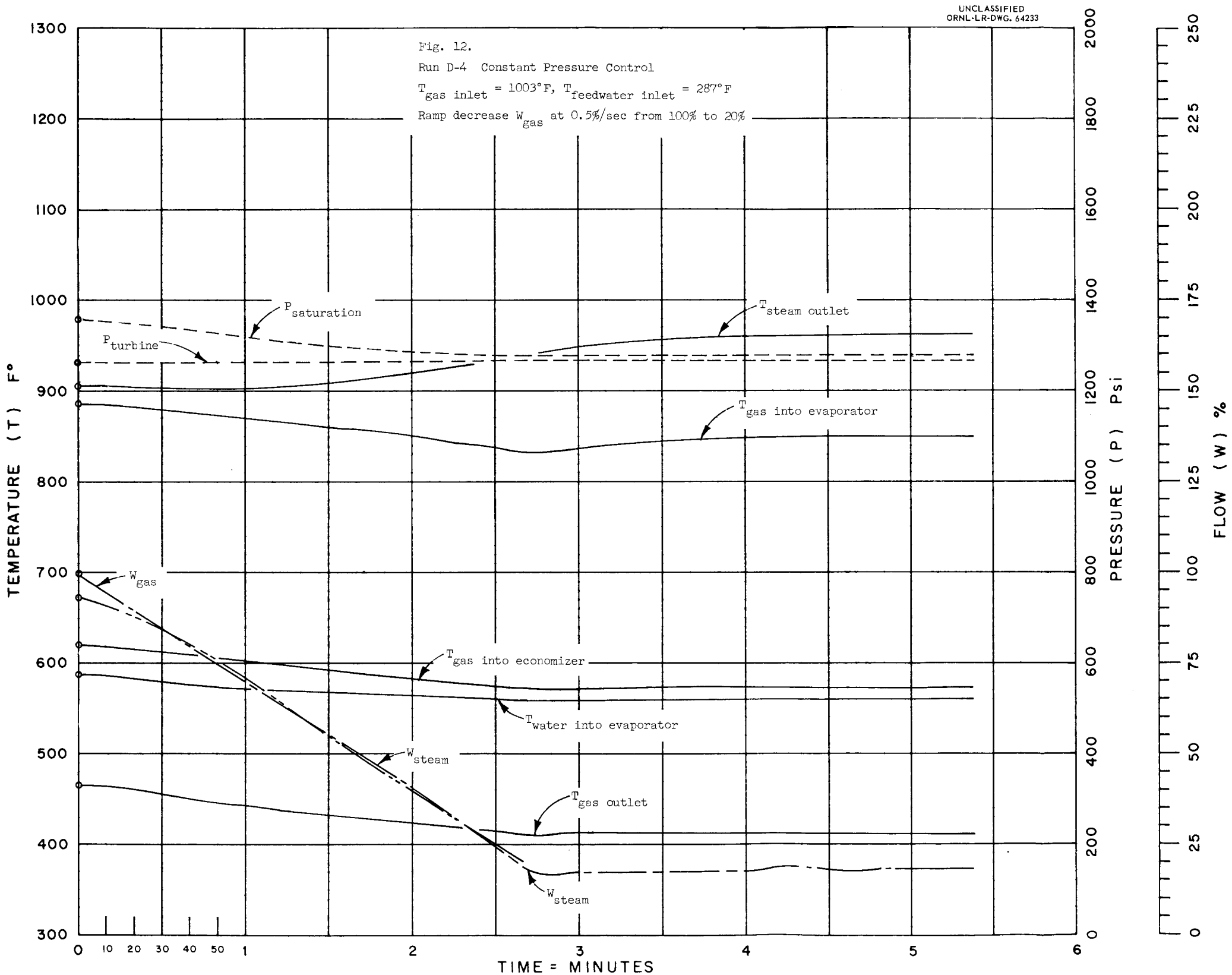
UNCLASSIFIED
ORNL-LR-DWG. 64233
Fig. 12.
Run D-4 Constant Pressure Control
$T_{gas\ inlet}$ = 1003°F, $T_{feedwater\ inlet}$ = 287°F
Ramp decrease W_{gas} at 0.5%/sec from 100% to 20%
$P_{saturation}$
$P_{turbine}$
$T_{steam\ outlet}$
$T_{gas\ into\ evaporator}$
W_{gas}
$T_{gas\ into\ economizer}$
$T_{water\ into\ evaporator}$
W_{steam}
$T_{gas\ outlet}$
W_{steam}
TEMPERATURE (T) F°
PRESSURE (P) Psi
FLOW (W) %
TIME = MINUTES
1300
1200
1100
1000
900
800
700
600
500
400
300
2000
1800
1600
1400
1200
1000
800
600
400
200
0
250
225
200
175
150
125
100
75
50
25
0
0
10
20
30
40
50
1
2
3
4
5
6

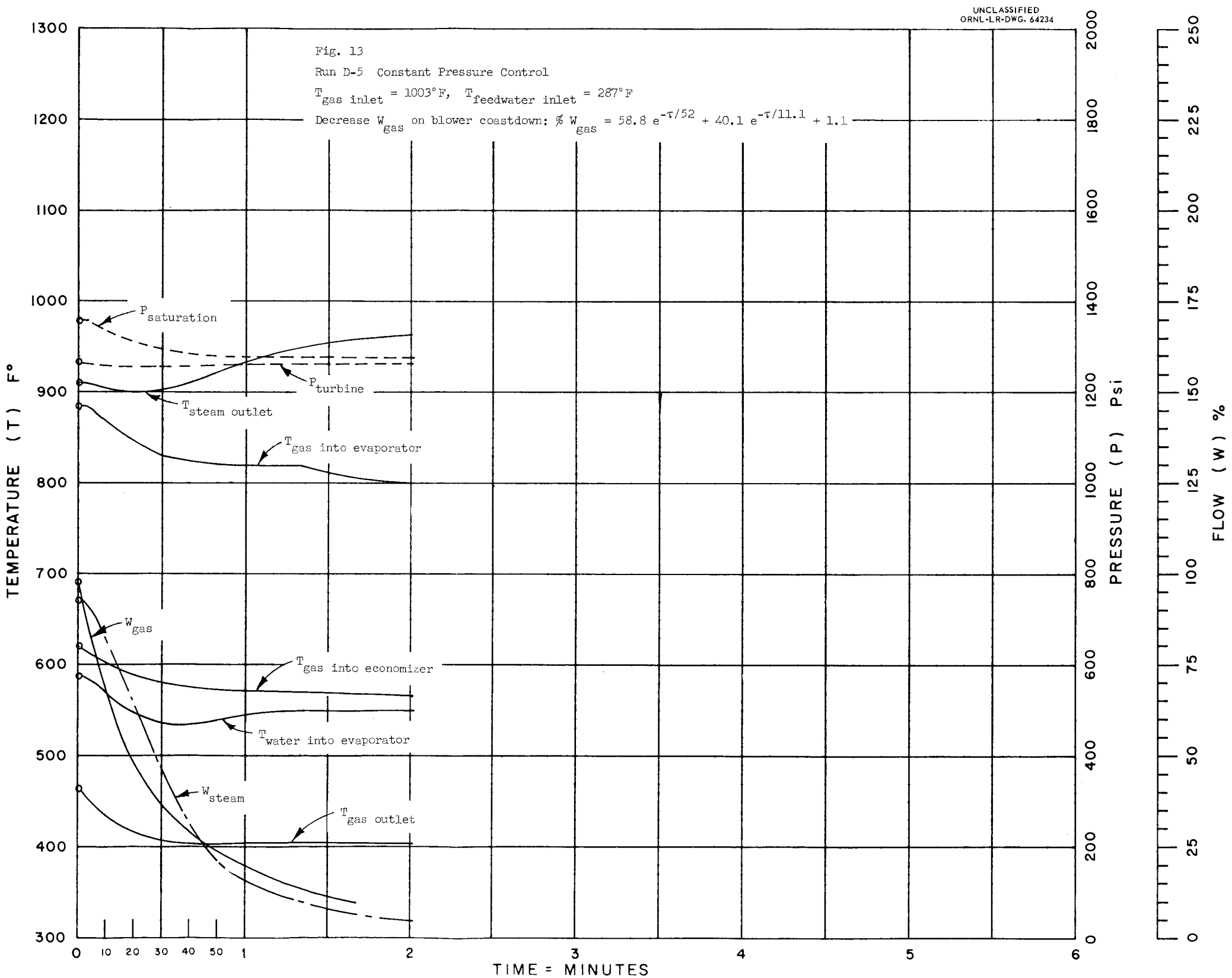
UNCLASSIFIED
ORNL-LR-DWG. 64234
Fig. 13
Run D-5 Constant Pressure Control
$T_{gas\ inlet}$ = 1003°F, $T_{feedwater\ inlet}$ = 287°F
Decrease W_{gas} on blower coastdown: % W_{gas} = 58.8 $e^{-\tau/52}$ + 40.1 $e^{-\tau/11.1}$ + 1.1
$P_{saturation}$
$P_{turbine}$
$T_{steam\ outlet}$
$T_{gas\ into\ evaporator}$
W_{gas}
$T_{gas\ into\ economizer}$
$T_{water\ into\ evaporator}$
W_{steam}
$T_{gas\ outlet}$
TEMPERATURE (T) F°
PRESSURE (P) Psi
FLOW (W) %
TIME = MINUTES

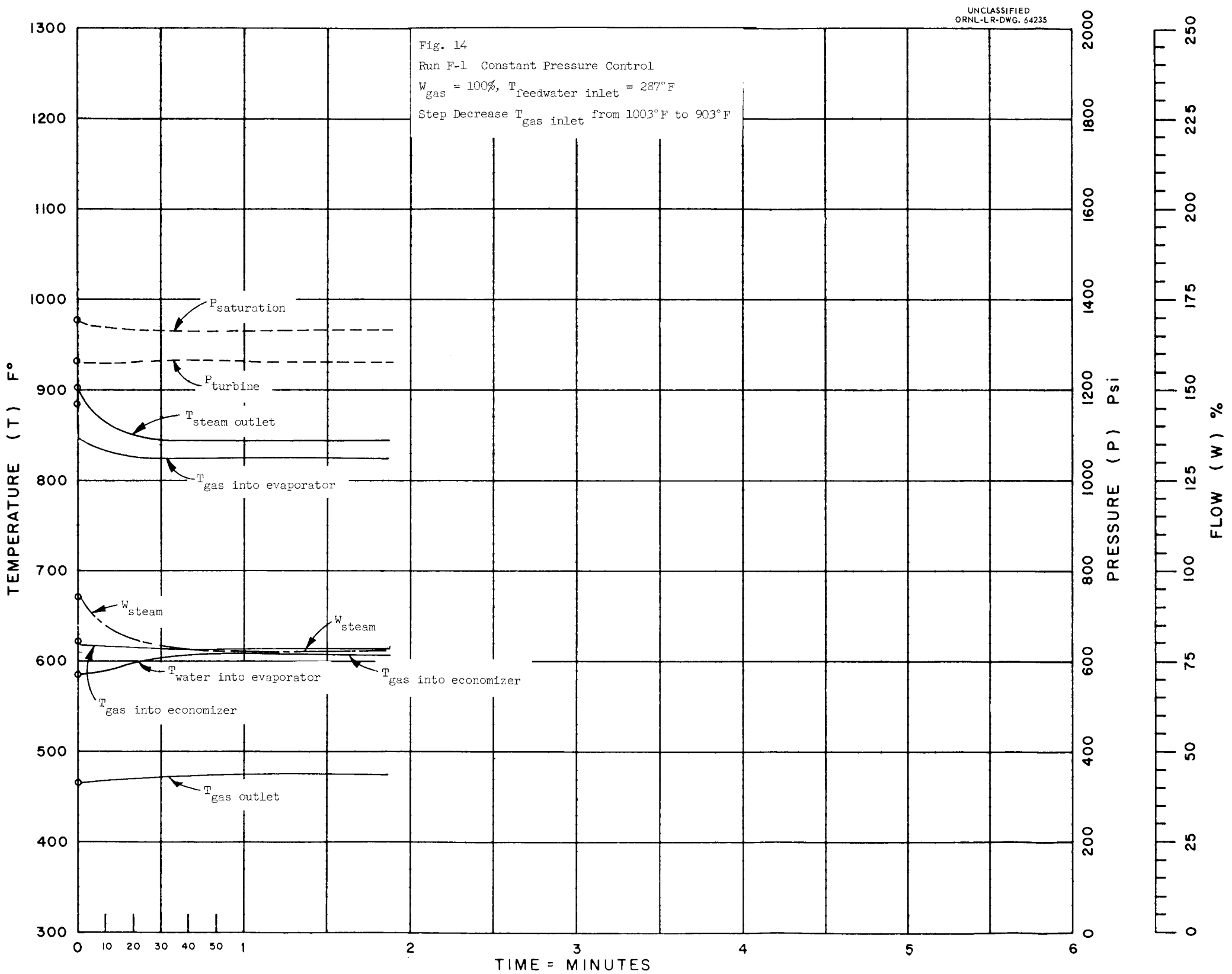
UNCLASSIFIED
ORNL-LR-DWG. 64235
Fig. 14
Run F-1 Constant Pressure Control
W_{gas} = 100%, $T_{feedwater\ inlet}$ = 287°F
Step Decrease $T_{gas\ inlet}$ from 1003°F to 903°F
$P_{saturation}$
$P_{turbine}$
$T_{steam\ outlet}$
$T_{gas\ into\ evaporator}$
W_{steam}
W_{steam}
$T_{water\ into\ evaporator}$
$T_{gas\ into\ economizer}$
$T_{gas\ into\ economizer}$
$T_{gas\ outlet}$
TEMPERATURE (T) F°
PRESSURE (P) Psi
FLOW (W) %
TIME = MINUTES
1300
1200
1100
1000
900
800
700
600
500
400
300
2000
1800
1600
1400
1200
1000
800
600
400
200
0
250
225
200
175
150
125
100
75
50
25
0
0
10
20
30
40
50
1
2
3
4
5
6

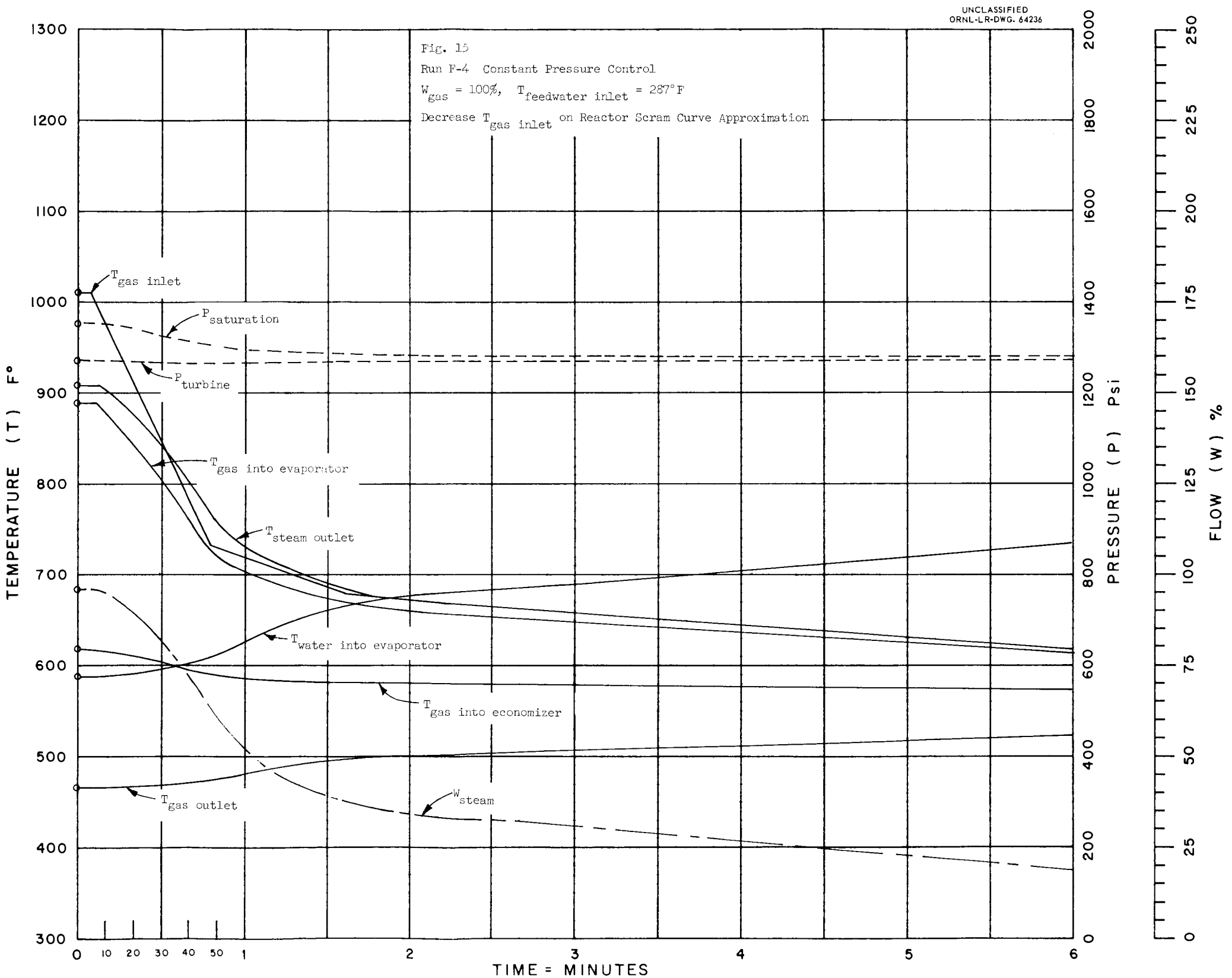
UNCLASSIFIED
ORNL-LR-DWG. 64236
Fig. 15
Run F-4 Constant Pressure Control
W_{gas} = 100%, $T_{feedwater\ inlet}$ = 287°F
Decrease $T_{gas\ inlet}$ on Reactor Scram Curve Approximation
$T_{gas\ inlet}$
$P_{saturation}$
$P_{turbine}$
$T_{gas\ into\ evaporator}$
$T_{steam\ outlet}$
$T_{water\ into\ evaporator}$
$T_{gas\ into\ economizer}$
$T_{gas\ outlet}$
W_{steam}
TEMPERATURE (T) F°
PRESSURE (P) Psi
FLOW (W) %
TIME = MINUTES
1300
1200
1100
1000
900
800
700
600
500
400
300
2000
1800
1600
1400
1200
1000
800
600
400
200
0
250
225
200
175
150
125
100
75
50
25
0
0
10
20
30
40
50
1
2
3
4
5
6

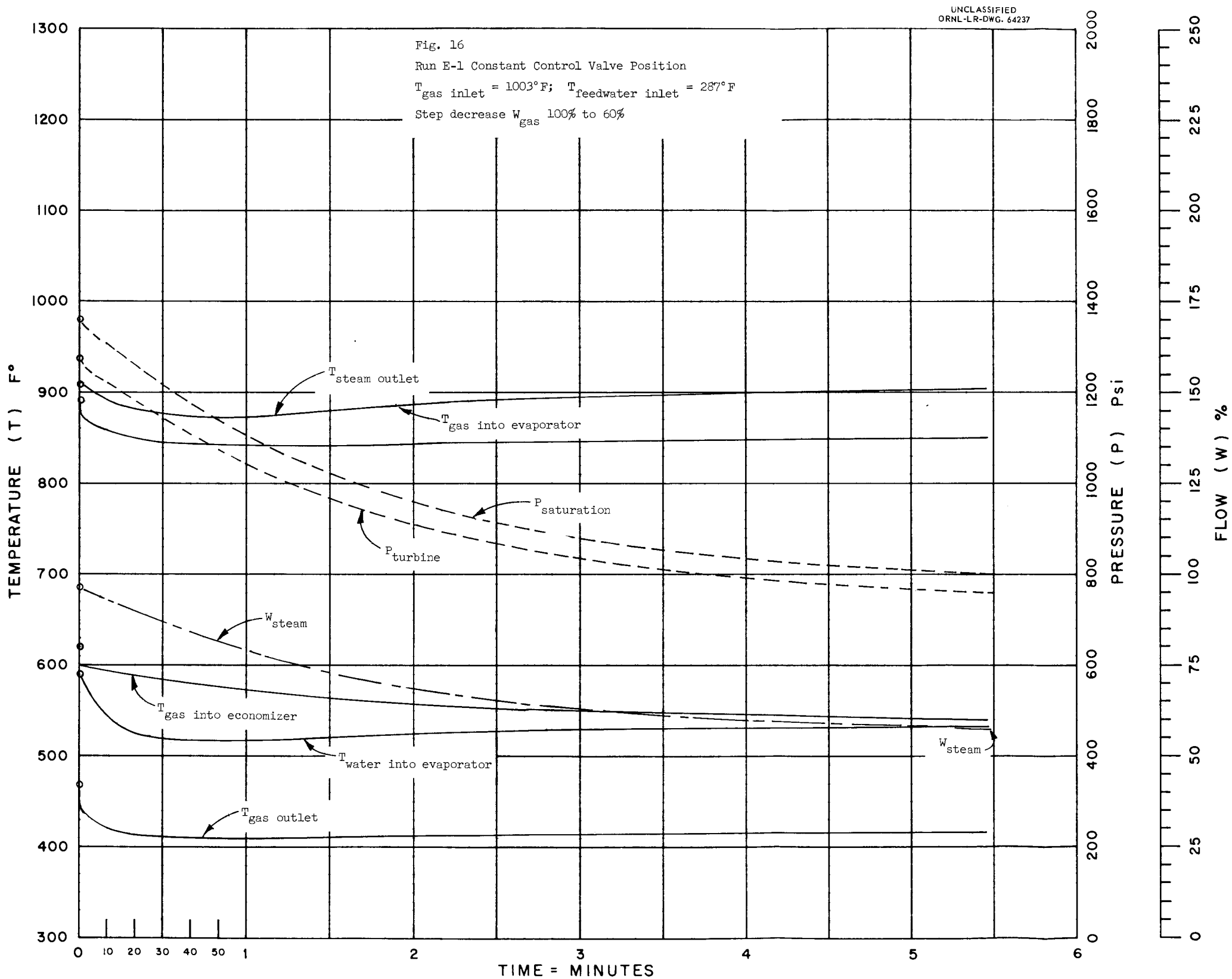
UNCLASSIFIED
ORNL-LR-DWG. 64237
Fig. 16
Run E-1 Constant Control Valve Position
$T_{gas\ inlet}$ = 1003°F; $T_{feedwater\ inlet}$ = 287°F
Step decrease W_{gas} 100% to 60%
$T_{steam\ outlet}$
$T_{gas\ into\ evaporator}$
$P_{saturation}$
$P_{turbine}$
W_{steam}
$T_{gas\ into\ economizer}$
$T_{water\ into\ evaporator}$
$T_{gas\ outlet}$
TEMPERATURE (T) F°
PRESSURE (P) Psi
FLOW (W) %
TIME = MINUTES
1300
1200
1100
1000
900
800
700
600
500
400
300
2000
1800
1600
1400
1200
1000
800
600
400
200
0
250
225
200
175
150
125
100
75
50
25
0
0
10
20
30
40
50
1
2
3
4
5
6

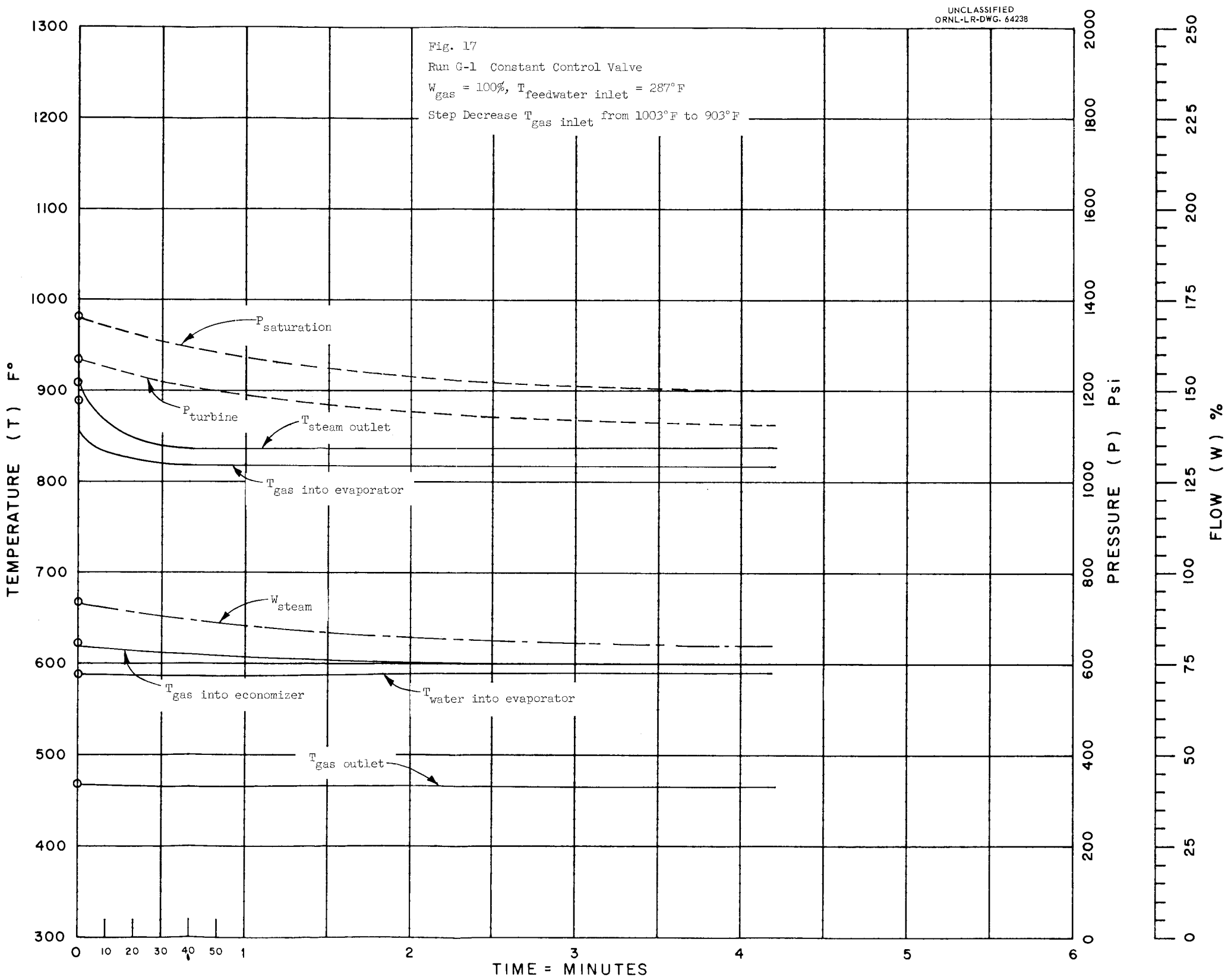
UNCLASSIFIED
ORNL-LR-DWG. 64238
Fig. 17
Run G-1 Constant Control Valve
W_{gas} = 100%, $T_{feedwater\ inlet}$ = 287°F
Step Decrease $T_{gas\ inlet}$ from 1003°F to 903°F
$P_{saturation}$
$P_{turbine}$
$T_{steam\ outlet}$
$T_{gas\ into\ evaporator}$
W_{steam}
$T_{gas\ into\ economizer}$
$T_{water\ into\ evaporator}$
$T_{gas\ outlet}$
TEMPERATURE (T) F°
PRESSURE (P) Psi
FLOW (W) %
TIME = MINUTES
1300
1200
1100
1000
900
800
700
600
500
400
300
2000
1800
1600
1400
1200
1000
800
600
400
200
0
250
225
200
175
150
125
100
75
50
25
0
0
10
20
30
40
50
1
2
3
4
5
6

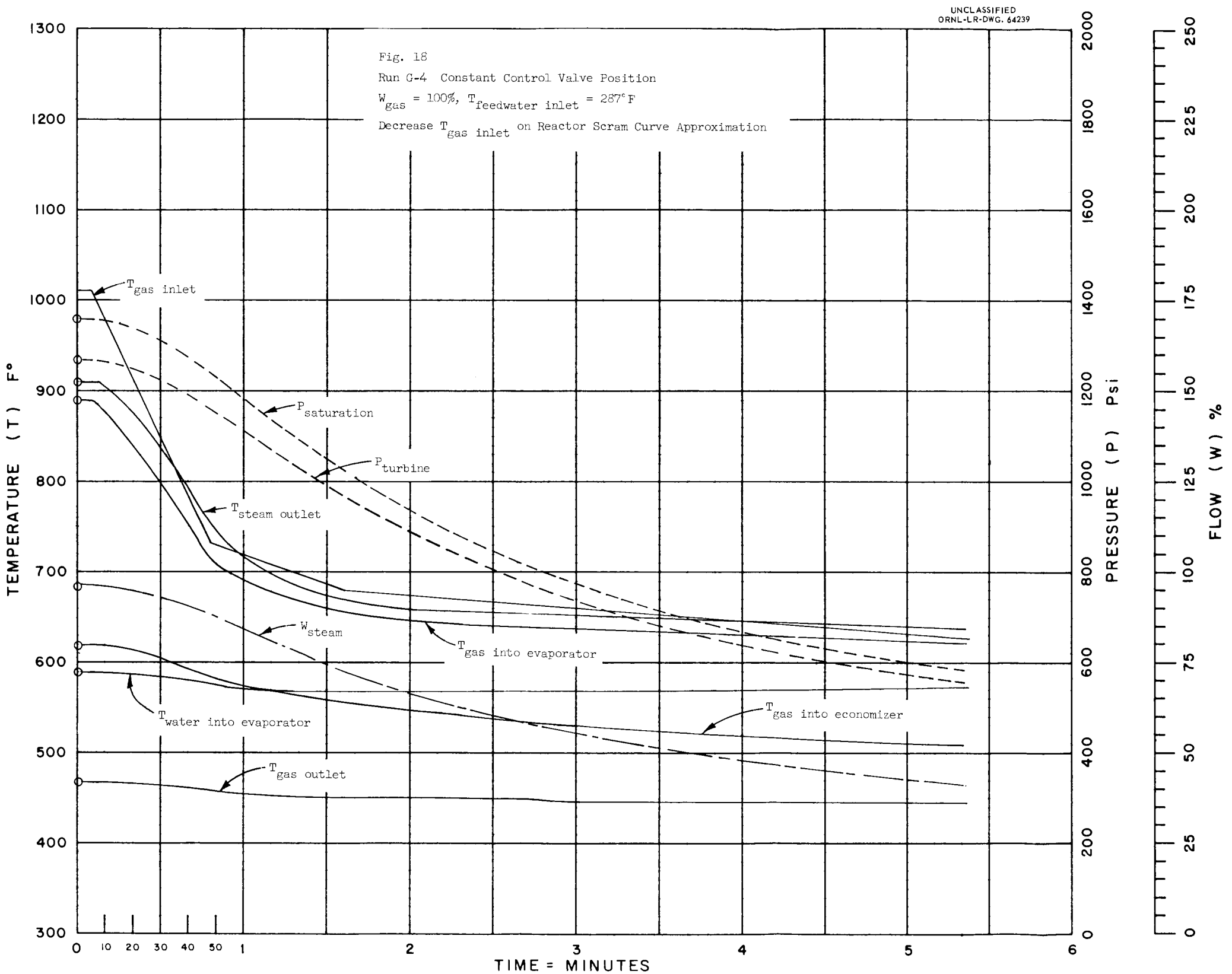
UNCLASSIFIED
ORNL-LR-DWG. 64239
Fig. 18
Run G-4 Constant Control Valve Position
W_{gas} = 100%, $T_{feedwater\ inlet}$ = 287°F
Decrease $T_{gas\ inlet}$ on Reactor Scram Curve Approximation
$T_{gas\ inlet}$
$P_{saturation}$
$P_{turbine}$
$T_{steam\ outlet}$
W_{steam}
$T_{gas\ into\ evaporator}$
$T_{water\ into\ evaporator}$
$T_{gas\ into\ economizer}$
$T_{gas\ outlet}$
TEMPERATURE (T) F°
PRESSURE (P) Psi
FLOW (W) %
TIME = MINUTES
1300
1200
1100
1000
900
800
700
600
500
400
300
2000
1800
1600
1400
1200
1000
800
600
400
200
0
250
225
200
175
150
125
100
75
50
25
0
0
10
20
30
40
50
1
2
3
4
5
6

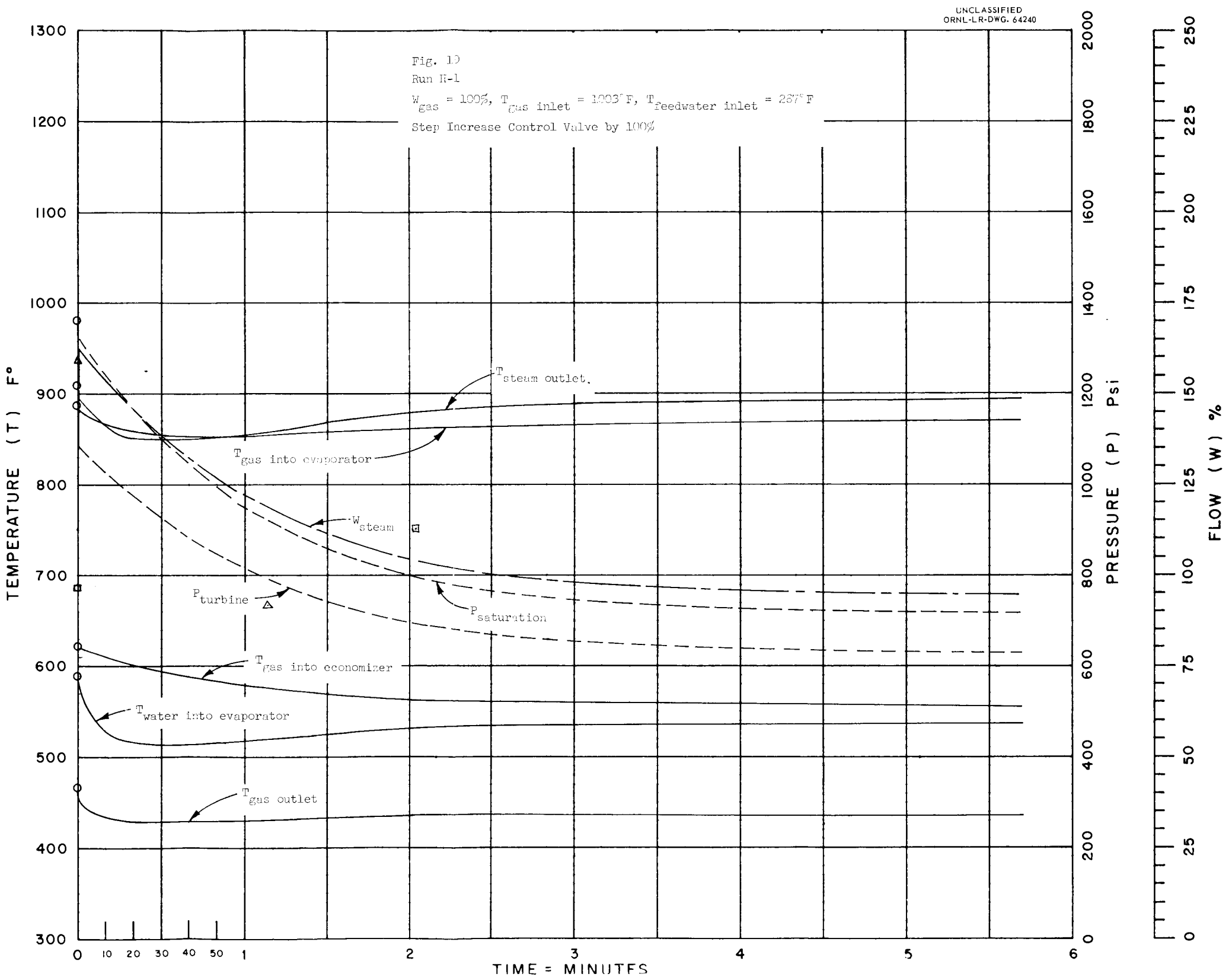
UNCLASSIFIED
ORNL-LR-DWG. 64240
Fig. 10
Run R-1
W_{gas} = 100%, $T_{gas\ inlet}$ = 1003°F, $T_{feedwater\ inlet}$ = 287°F
Step Increase Control Valve by 100%
$T_{steam\ outlet}$
$T_{gas\ into\ evaporator}$
W_{steam}
$P_{turbine}$
$P_{saturation}$
$T_{gas\ into\ economizer}$
$T_{water\ into\ evaporator}$
$T_{gas\ outlet}$
TEMPERATURE (T) F°
PRESSURE (P) Psi
FLOW (W) %
TIME = MINUTES
1300
1200
1100
1000
900
800
700
600
500
400
300
2000
1800
1600
1400
1200
1000
800
600
400
200
0
250
225
200
175
150
125
100
75
50
25
0
0
10
20
30
40
50
1
2
3
4
5
6

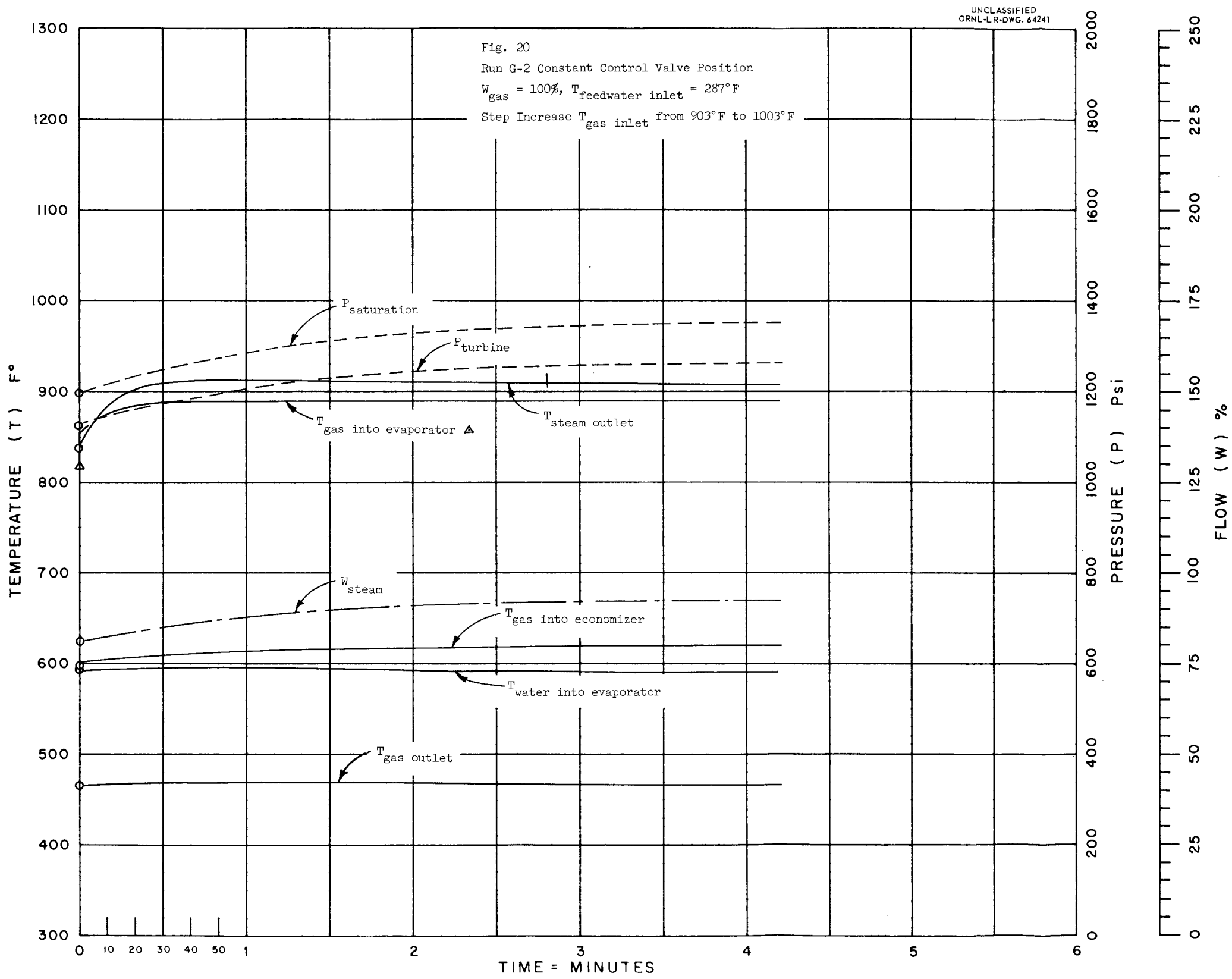
UNCLASSIFIED
ORNL-LR-DWG. 64241
Fig. 20
Run G-2 Constant Control Valve Position
W_{gas} = 100%, $T_{feedwater\ inlet}$ = 287°F
Step Increase $T_{gas\ inlet}$ from 903°F to 1003°F
$P_{saturation}$
$P_{turbine}$
$T_{gas\ into\ evaporator}$
$T_{steam\ outlet}$
W_{steam}
$T_{gas\ into\ economizer}$
$T_{water\ into\ evaporator}$
$T_{gas\ outlet}$
TEMPERATURE (T) F°
PRESSURE (P) Psi
FLOW (W) %
TIME = MINUTES
1300
1200
1100
1000
900
800
700
600
500
400
300
2000
1800
1600
1400
1200
1000
800
600
400
200
0
250
225
200
175
150
125
100
75
50
25
0
0
10
20
30
40
50
1
2
3
4
5
6

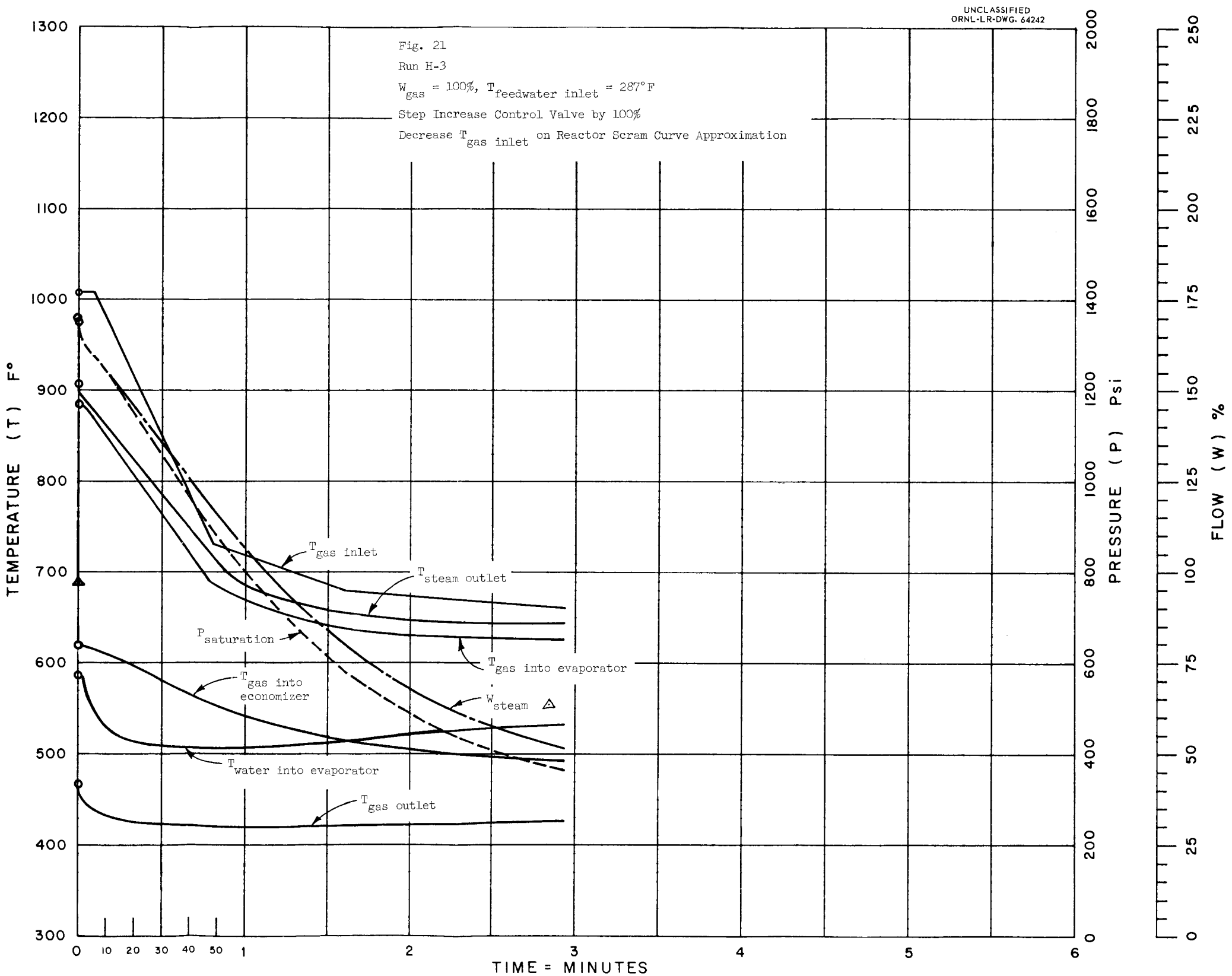
UNCLASSIFIED
ORNL-LR-DWG. 64242
Fig. 21
Run H-3
W_{gas} = 100%, $T_{feedwater\ inlet}$ = 287°F
Step Increase Control Valve by 100%
Decrease $T_{gas\ inlet}$ on Reactor Scram Curve Approximation
TEMPERATURE (T) F°
PRESSURE (P) Psi
FLOW (W) %
TIME = MINUTES
$T_{gas\ inlet}$
$T_{steam\ outlet}$
$P_{saturation}$
$T_{gas\ into\ evaporator}$
$T_{gas\ into\ economizer}$
W_{steam}
$T_{water\ into\ evaporator}$
$T_{gas\ outlet}$

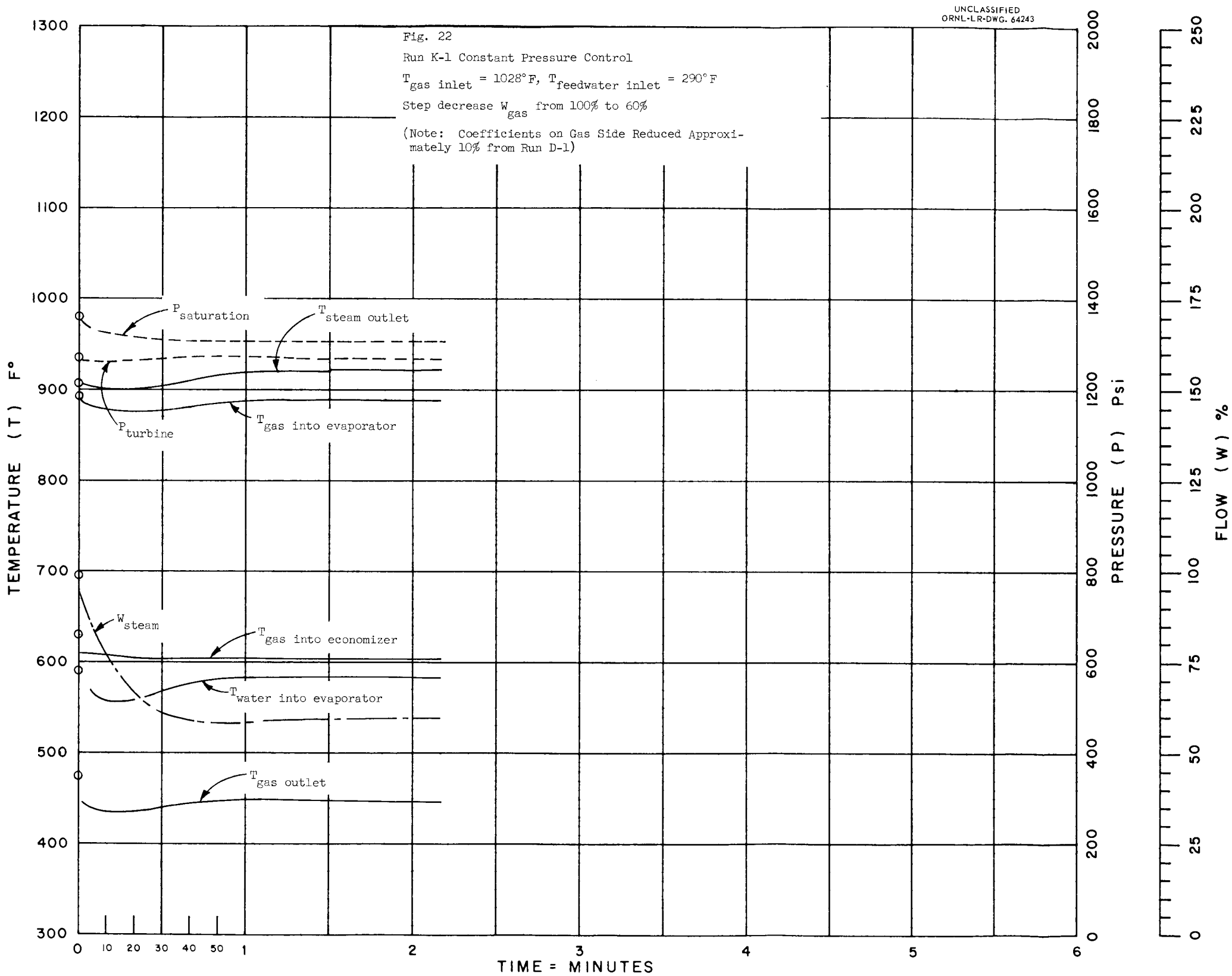
UNCLASSIFIED
ORNL-LR-DWG. 64243
Fig. 22
Run K-1 Constant Pressure Control
$T_{gas\ inlet}$ = 1028°F, $T_{feedwater\ inlet}$ = 290°F
Step decrease W_{gas} from 100% to 60%
(Note: Coefficients on Gas Side Reduced Approximately 10% from Run D-1)
$P_{saturation}$
$T_{steam\ outlet}$
$P_{turbine}$
$T_{gas\ into\ evaporator}$
W_{steam}
$T_{gas\ into\ economizer}$
$T_{water\ into\ evaporator}$
$T_{gas\ outlet}$
TEMPERATURE (T) F°
PRESSURE (P) Psi
FLOW (W) %
TIME = MINUTES
1300
1200
1100
1000
900
800
700
600
500
400
300
2000
1800
1600
1400
1200
1000
800
600
400
200
0
250
225
200
175
150
125
100
75
50
25
0
0
10
20
30
40
50
1
2
3
4
5
6

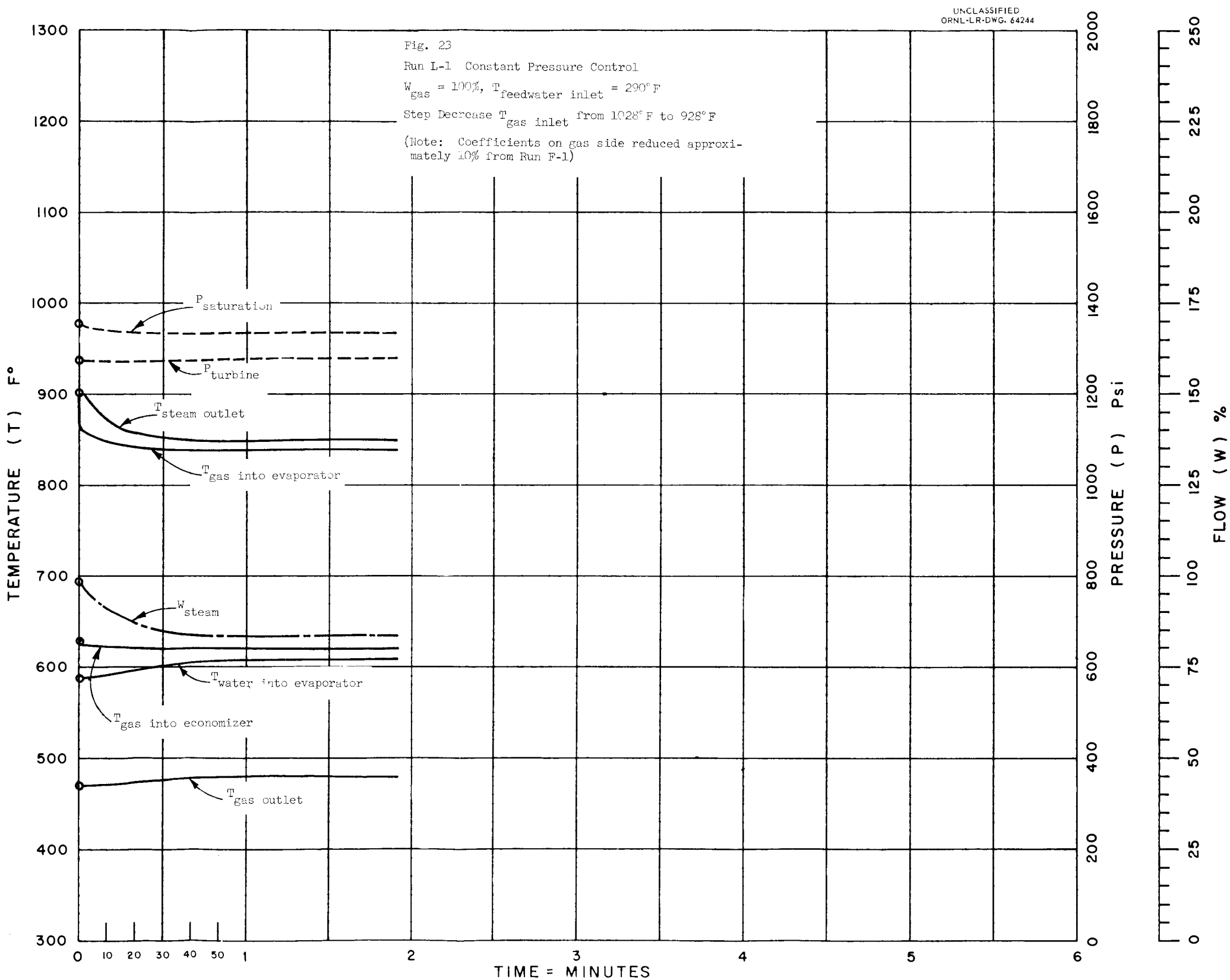
UNCLASSIFIED
ORNL-LR-DWG. 64244
Fig. 23
Run L-1 Constant Pressure Control
W_{gas} = 100%, $T_{feedwater\ inlet}$ = 290° F
Step Decrease $T_{gas\ inlet}$ from 1028° F to 928° F
(Note: Coefficients on gas side reduced approximately 10% from Run F-1)
$P_{saturation}$
$P_{turbine}$
$T_{steam\ outlet}$
$T_{gas\ into\ evaporator}$
W_{steam}
$T_{water\ into\ evaporator}$
$T_{gas\ into\ economizer}$
$T_{gas\ outlet}$
TEMPERATURE (T) F°
PRESSURE (P) Psi
FLOW (W) %
TIME = MINUTES
1300
1200
1100
1000
900
800
700
600
500
400
300
2000
1800
1600
1400
1200
1000
800
600
400
200
0
250
225
200
175
150
125
100
75
50
25
0
0
10
20
30
40
50
1
2
3
4
5
6

TABLE II

Summary of Series Runs on Analog Study

Series	Run	Operating Conditions or Perturbations	Figure No.	Page
A	1	Steady state, 903°F steam, 100% gas flow	8	25
	2	80% gas flow	8	25
	3	60% gas flow	8	25
	4	40% gas flow	8	25
		20% gas flow	8	25
B	1	Steady state, 1043°F, gas 100% gas flow	9	26
	2	80% gas flow	9	26
	3	60% gas flow	9	26
	4	40% gas flow	9	26
	5	20% gas flow	9	26
D	1	Constant pressure control: step decrease gas flow 100-60%	11	28
	2	step increase gas flow 60-100%	A-1	62
	3	step decrease gas flow 100-20%	A-2	63
	4	ramp gas flow at 0.5%/sec to 20%	12	29
	5	decrease gas flow on Kaiser blower coastdown curve	13	30
E	1	Constant position of steam control valve: step decrease gas flow 100-60%	16	33
	2	Constant position of steam control valve: step increase gas flow 60-100%	A-3	64

TABLE II (continued)

Series	Run	Operating Conditions or Perturbations	Figure No.	Page
F	1	Constant pressure control: step decrease gas temperature 1003-903°F	14	31
	2	step increase gas temperature 903-1003°F	A-4	65
	4	decrease gas temperature approximating reactor scram	15	32
	5	step increase gas temperature 985-1085°F with 60% gas flow	A-5	68
	6	step increase gas temperature 932-1032°F with 20% gas flow	A-6	67
G	1	Constant position of steam control valve: step decrease gas temperature 1003-903°F	17	34
	2	step increase gas temperature 903-1003°F	20	37
	4	decrease gas temperature approximating reactor scram	18	35
	5	Step control valve open on decrease of gas temperature approximating reactor scram	A-7	66
H	1	Step increase control valve opening by 100%	19	36
	2	Step increase control valve opening by 100%, decrease gas flow on blower coastdown	A-8	69
	3	decrease gas temperature approximating reactor scram	21	38

TABLE II (continued)

Series	Run	Operating Conditions or Perturbations	Figure No.	Page
K	1	Constant pressure control: step decrease of gas flow using a reduced gas coefficient	22	39
L	1	Constant pressure control: step decrease gas temperature using a reduced gas coefficient	23	40

change of gas flow from 100 to 60% was made at time zero with the steam turbine under pressure regulator control. Although it is not anticipated that step changes of this magnitude will occur in operation, such changes are useful in an analysis of the transient response of the system.

The step decrease in gas flow causes an instantaneous step reduction in the gas-side coefficient which is proportional to approximately the 0.61 power of flow. Since the temperature drop of a fluid passing over a cooling surface is proportional to the heat transfer rate divided by the fluid flow rate, one can see that a decrease in flow rate initially would cause a decrease in the gas outlet temperature. Because no transport lag for the gas flow through the steam generator is included in the simulation, the model shows the drop in gas temperatures out of the three steam generator regions to be instantaneous.

The reduction in the gas heat load results in a drop in the rate of steam generation. Examination of Run D-1 shows the saturation pressure dropping off. This is because the reduced steam flow (i.e., steam generation) results in a reduced pressure drop between the evaporator and the turbine valve where the steam pressure is held constant. The reduction in steam flow (and thus feedwater flow) results in reduced economizer and superheater heat transfer coefficients, and this further reduces the heat transfer capacity of the steam generator. Thus there is a gradual increase in the gas-side temperatures to a new equilibrium condition.

The initial drop in steam outlet temperature due to the reduced gas-side load is eventually recovered because of the subsequent reduction in steam flow rate, and thus the final steam outlet temperature is above the initial value. In a similar manner, the initial fall and subsequent rise of the evaporator water inlet temperatature reflects the initial effect of reduced gas heat load and subsequent reduction in feedwater flow rate.

Run D-4 (Fig. 12) shows the transient effects of a ramp change in gas flow rate from 100 to 20% at 0.5%/sec.

Run D-5 (Fig. 13) simulates a blower scram with a constant gas temperature entering the steam generator. This condition approximates an actual simultaneous reactor and blower scram. It should be noted that in the first 15 sec the rate of change of the steam generator gas outlet temperature exceeds the maximum specified rate of temperature change of 150°F/min given in the steam generator specification PJ-1. Note also that during the coastdown period of the blowers the steam outlet temperature rises to between 950 and 975°F and may remain in that temperature range for a period exceeding that specified in the steam generator specification. (The latter states that the maximum steam temperature may be 950 to 975°F but for no greater than a 15-min duration and must aggregate no more than 1% of the total operating time in this temperature range.) When the turbine is removed from the line, however, and the pressure is no longer controlled, an increase in the steam flow (via the dump) will reduce the steam temperature.

2. Inlet Gas Temperature Change

The effect of a step change in gas temperature with the turbine under pressure control is shown in Fig. 14, Run F-1. Here the gas inlet temperature was reduced 100°F. The temperatures of the gas entering both the evaporator and economizer sections show step changes since no transport lag was included in the model. The magnitude of these step changes is significantly reduced, however, since the capacity of each section of the steam generator is reduced as a function of the change in log mean temperature driving force.

The gas temperature leaving the steam generator increases slightly with lower inlet gas temperatures. This results from the reduction in steam generator capacity which occurs because of the lower temperature driving force in the steam generator

and the subsequent reduction in steam flow rate and tube-side heat transfer coefficient. It is important to recognize that the effect of the turbine pressure regulator is to accelerate the reduction in steam-side flow in order to maintain a constant turbine throttle pressure under conditions of reduced gas flow or gas temperature.

The effect of a more complex reduction in gas temperature is shown in Fig. 15, Run F-4, using an approximation to the gas temperature leaving the reactor on a reactor scram with the blowers in continued operation. Behavior of the gas temperature through the unit was similar to the case in Run F-1, the step reduction in inlet temperature. There exists, however, an unbalanced condition of gas temperature entering the economizer well below the water temperature leaving the economizer, and the transient traces through the 6 min of operation indicated no return to equilibrium conditions. The physical interpretation of this is that during the transient at reduced gas inlet temperature, there is a shifting of the boiling region within the steam generator into the economizer section. The graph at 6 min shows a saturation pressure of 1280 psia which corresponds to a temperature of 576°F, while the water temperature entering the evaporator section is indicated to be 735°F. The rapid drop in gas inlet temperature reduces saturation pressure and results in a reduced steam-side flow and reduced superheated steam heat transfer coefficient. The drop in superheater capacity because of the reduced heat transfer coefficient and reduced temperature driving force tends to shift the heat load to the evaporator and economizer sections. The analog simulation in the economizer utilizes a forced heat balance and requires that the heat transfer all occur as sensible heat increase of the water. Thus the water temperature leaving the economizer is a fictitious value under these conditions and indicates that boiling would actually occur in the economizer.

Note that the steep inlet temperature gradient is greatly damped within the unit so that response on the outlet gas temperature is not sharp. In the run discussed, the outlet gas temperature shows about a 10-deg rise 45 sec after the initial perturbation and after the gas inlet temperature has dropped approximately 280°F. This indicates the extreme insensitivity of steam generator gas outlet temperature to steam generator gas inlet temperature. During the transient period, outlet gas temperature rises about 60°F over the 6-min trace period.

It should be recalled that initial conditions for the simulation were intended to be maintained between 20 to 100% power conditions. Steam conditions were assumed not to deviate greatly from the design conditions so that assumptions on thermodynamic properties of steam and latent heat of vaporization are less valid at conditions far from design.

Note that even with very low steam flows the turbine throttle pressure can be maintained for several minutes after initiation of a scram. The traces showed no evidence of turbine pressure deterioration. This should aid in determining when the turbine need be removed from the line in the event of a reactor scram.

C. Turbine Control Valve Position Constant

To simulate the effect on steam flow of a turbine regulated under speed control, a number of transient runs were conducted while maintaining the control valve opening at a constant position. Tests were also conducted making step changes in the control valve position.

1. Perturbations to Gas Flow

Figure 16, Run E-1, shows the effect of a step change in gas flow from 100 to 60% with a constant control valve opening. The reduced gas flow and gas heat transfer coefficient again cause an

instantaneous drop in gas temperatures leaving each section of the steam generator. This time, however, with no pressure regulation, the saturation pressure and turbine throttle pressure both decrease with the reduced steam flow rate. The initial drop in steam temperature due to reduced heat transfer is reversed at lower steam flows, and the steam temperature gradually rises. The combined effect of reduced heat transfer due to lower steam and gas flows and increasing steam temperature reduces the superheater capacity and results in a slowly increasing gas temperature leaving the superheater.

The effect on the evaporator section is not as pronounced. The drop in saturation pressure reduces the evaporator temperature, and since the tube-side coefficient in the evaporator is unaffected by steam-side flow, the gas temperature leaving the evaporator continues to decrease. The economizer section responds somewhat like the superheater in initially suffering a decrease in capacity because of a reduced temperature driving force and reduced heat transfer coefficient. Since, however, the gas temperature entering the economizer is dropping in temperature, an almost constant gas discharge temperature occurs after the initial 20 sec of the transient.

2. Perturbations to Gas Temperature

The effect of a 100°F step decrease in gas inlet temperature with a constant control valve position is shown in Fig. 17, Run G-1. Comparison of Fig. 14 with Fig. 17, Run F-1 (with pressure control) with G-1, shows remarkably similar response characteristics between the two transients. The essential difference lies in the continued decrease of turbine and evaporator pressures and of steam flow over the interval considered in the case of the constant control valve position. The effect on gas outlet temperature was negligible in both cases.

A simulation of a reactor scram with the blowers remaining on is shown in Fig. 18, Run G-4. In this case steam generator gas inlet temperature was decreased as shown on the figure with the control valve held constant. The graph shows a rapid deterioration of turbine and saturation pressures but again a relatively stable gas outlet temperature. The reversal of water temperature leaving the economizer and gas temperature entering is again shown, indicating that boiling is occurring in the economizer section. Note that in this case the outlet gas temperature from the steam generator decreases slightly during a reactor scram, while with the system under pressure regulator control the gas temperature increases slightly for this scram condition. The difference is due to the effect on the heat transfer coefficient and water temperature of the much reduced water flow with the turbine under pressure regulator control. Note that the direction of change of outlet gas temperature with a given change of gas inlet temperature appears to be a function of the type of control of the throttle valve.

3. Perturbations in Turbine Throttle Valve Opening

The effect of a step change in the control valve opening was simulated in Run H-1 shown in Fig. 19. A step increase of 100% in valve opening causes an instantaneous change in steam flow rate (and hence water flow rate), resulting in a drop in the bulk gas temperatures in the heat exchanger as a result of a higher heat removal rate. The unbalance between heat supply and removal rates results in a subsequent reduction in steam flow rate. As the steam flow rate is reduced, the initial reduction in steam temperature is partially recovered. The behavior of the economizer water outlet temperature is similar to that of the superheater steam outlet temperature. The evaporator capacity is increased by the reduction in saturation temperature and consequent increase

in pinch point temperature difference. The economizer and superheater capacities are reduced by the reduced heat transfer coefficients after the initial instantaneous rise in capacity.

The effect of a step change in throttle valve position simultaneously with a blower coastdown was examined in Run H-2, Fig. A-8. In this case a very rapid deterioration of steam conditions occurred. After the instantaneous increase steam flow drops off, and the graph indicates that the steam temperature begins to recover because of the drastic reduction in steam flow. Gas outlet temperature decreased at approximately 250°F/min for the first 30 sec of the transient. This case approximates a loss of electrical power. It assumes a constant temperature into the steam generator and simulates opening of the electromagnetic relief valves. In the case of a true loss of power, the gas inlet temperature may change somewhat, but as shown in Fig. 20, Run G-2, the effect of an increase in gas inlet temperature on gas outlet temperature under a constant valve position is slight. In the loss-of-power accident feedwater flow from the emergency surge drum was assumed to maintain the liquid level in the drum.

The condition of either a steam line rupture or opening of relief or electromagnetic valves on the steam system again imposes temperature transients on the steam generator in excess of those specified by PJ-1. Since the value used in the study for the increased opening for steam flow may be low, the actual transient may be more severe than that shown.

The effect of steam blowdown with a reactor scram with the blowers remaining on is shown in Fig. 21, Run H-3. Again a rapid deterioration of steam conditions occurs, but the effect on steam generator gas outlet temperature is much less severe. This is consistent with previous results already discussed.

4. Reduced Gas-Side Coefficient

To confirm the theory that small errors in computed heat transfer coefficients would have a negligible effect on the transient response of the steam generator, a reduction of approximately 10% on the gas coefficient was effected. Runs K-1 and L-1, Figs. 22 and 23 (showing step changes in gas flow and inlet temperature), may be compared with Figs. 11 and 14, Runs D-1 and F-1. The transient response was essentially identical in both cases. This indicates that possible errors in predicting accurate heat transfer coefficients should not jeopardize the validity of the analog transient response characteristics.

VI. Conclusions and Recommendations

1) Results of the study are reasonable, and the model appears to describe adequately the performance of the steam generator under the conditions of operation studied. The equilibrium operating conditions predicted from the simulator analysis agree well with hand calculations. The transient response of the system to perturbations can be logically explained.

2) Assuming good gas flow distribution across the tube matrix, the thermal capacity of the steam generator at full power conditions is adequate. It is probable that a steam generator inlet gas temperature lower than 1043°F will be required to hold a steam temperature of 903°F leaving the steam generator.

3) Several transient conditions can exist during which the rate of change of gas and/or steam temperature exceeds the value of 150°F/min specified in PJ-1 steam generator specifications. Since there are several critical areas in the steam generator which may be affected by such temperature transients, it is necessary to determine the implications of these transients on the present design.[7]

4) Remedial measures to reduce the gas temperature transient leaving the reactor during a scram must consider the effect on gas temperature leaving the steam generator. For example, the use of a braking mechanism for slowing the blowers down faster than the Kaiser blower coastdown curve will increase the temperature transient leaving the steam generator.

5) Gas temperature leaving the steam generator is insensitive to gas temperature changes entering the steam generator. The steam generator thermal capacity is large. Changes in the gas inlet temperature essentially affect only the temperature driving force to the sink temperature. The steam generator, because of its large thermal capacity, acts somewhat like an infinite sink. The effect of the

change in gas inlet temperature is largely absorbed by the steam generator unit and is not reflected by a change in gas outlet temperature. In addition, direction of response under certain conditions is dependent on whether the system is operating under turbine pressure regulator control or with the control valve position held constant. Thus with the system under a constant control valve setting, the steam generator gas outlet temperature decreases with a decrease in gas inlet temperature. Under the same conditions but with the steam system under pressure regulation, the outlet temperature increases with a drop in gas inlet temperature.

6) Under a condition of steam pressure regulation, steam temperatures rise on a reactor scram and may exceed the time-temperature limitations specified in PJ-1. The implications of this situation to the steam generator design should be examined.

7) The deterioration of steam pressure to the turbine with the turbine under pressure regulator control on a reactor scram is very gradual. Several minutes are available before the turbine need be tripped off the line because of low pressure.

Acknowledgment

The authors wish to acknowledge the helpful critical reviews of this paper by E. R. Mann and R. B. Korsmeyer.

Nomenclature

C_p	specific heat, Btu/lb-°F
C_v	valve seat opening
D	diameter, ft
d	diameter, in.
G	mass velocity, lb/ft^2-sec
G_{max}	maximum mass velocity
h	heat transfer coefficient, Btu/hr-ft^2-°F
j	j factor, $h/C_p G\ X(Pr)^{2/3}$, dimensionless
k	thermal conductivity, Btu/hr-ft-°F
L	length, ft
N	number of fins per inch
Nu	Nusselt number, hD/k, dimensionless
Pr	Prandtl number, $C_p\mu/k$, dimensionless
Re	Reynolds number, DG/μ, dimensionless
S	tube pitch for an equilateral triangular arrangement, in.
U	over-all heat transfer coefficient, Btu/hr-ft^2-°F
μ	viscosity, lb-mass/ft-sec

Subscripts

f	film or fin
i	inside
t	tube
e	equivalent

APPENDIX

Summary of Equations Used in Analog Model

1. Superheater Section

The superheater model is divided into three axial lumps, each solving the equations for: 1) heat transfer from the gas to the tubing, 2) heat storage in the tubing, and 3) heat transfer from the tubing to the steam.

The finite difference approximations to the heat transfer equations are of the form:

$$\frac{d\bar{T}_P}{dt} = K_1 (\bar{T}_G - \bar{T}_P) + K_2 (\bar{T}_S - \bar{T}_P) \qquad °F/sec$$

$$\bar{T}_G = T_{G(in)} - K_3 (\bar{T}_G - \bar{T}_P) \qquad °F$$

$$T_{G(out)} = \bar{T}_G - K_3 (\bar{T}_G - \bar{T}_P) \qquad °F$$

$$\bar{T}_S = T_{S(in)} + K_4 (\bar{T}_P - \bar{T}_S) \qquad °F$$

$$T_{S(out)} = \bar{T}_S + K_4 (\bar{T}_P - \bar{T}_S) \qquad °F$$

where

$\bar{T}_P$ = mean tubing temperature in lump
$\bar{T}_G$ = mean gas temperature in lump
$\bar{T}_S$ = mean steam temperature in lump
$T_{G(in)}$ = temperature of gas entering lump
$T_{G(out)}$ = temperature of gas leaving lump
$T_{S(in)}$ = temperature of steam entering lump
$T_{S(out)}$ = temperature of steam leaving lump
K_1, K_2, K_3, K_4 = see Table III

TABLE III

Tabulation of "K" Symbols Used in Equations Describing Analog Model

Superheater Section			Value at 100% Flow			
Symbol	Units	Represents	Lump 1	Lump 2	Lump 3	Varies as
K_1	sec^{-1}	$h_G A_G / M_P C_P$	0.0790	0.0689	0.0602	$W_G^{0.61}$
K_2	sec^{-1}	$h_S A_S / M_P C_P$	0.1020	0.1134	0.1225	$W_S^{0.8}$
K_3	Dl	$h_G A_G / 2W_G C_G$	0.1590	0.1386	0.1641	$W_G^{-0.39}$
K_4	Dl	$h_S A_S / 2W_S C_S$	0.7350	0.7120	0.6620	$W_S^{-0.2}$

Evaporator and Economizer Sections

Symbol	Units	Represents	Value (100% Flow)	Varies as	Reference
K_5	Dl	$\frac{\% \Delta T}{T_{G(in)} - T_{SAT}}$	86.8	W_G	Fig. A-14
K_6	$[(psi)(sec^2)]/(lb)^2$	flow resistance	0.0714		
K_7	$[(psi)(sec)]/(lb)$	valve factor	32.5		
K_8	lb/°F-sec	water instability factor	large positive number		
K_9	lb/Btu	$1/h_{fg}$	0.00173	$T_{W(evap)}$	Fig. A-9
K_{10}	Dl	heat transfer factor	0.181	$W_G^{-0.39}$, ΔU factor	
K_{11}	Dl	heat transfer factor	0.634	$W_G^{-0.39}$, ΔU factor	

The steam-side heat transfer coefficients given include the tube resistance and fouling resistance.

The time lag circuits used to multiply $(\bar{T}_P - \bar{T}_S)$ by 2 have no physical significance. They are included to dampen spurious oscillations arising from algebraic loop problems.[8]

A mathematical development of the finite difference approximations used is given in ORNL CF-60-9-116.[9]

2. Evaporator Section

The equation for the change in gas temperature through the evaporator is:

$$\Delta T_{G(evap)} = [T_{G(in)} - T_{SAT}]\, K_5 \qquad °F$$

where

$K_5 = \% \, \Delta T_G / [T_{G(in)} - T_{SAT}]$, as shown in Fig. A-14

Also,

$$T_{G(out)} = T_{G(in)} - \Delta T_{G(evap)} \qquad °F$$

The power input to the evaporator water and metal from the gas:

$$\text{Evap power} = W_G \, C_G \, \Delta T_{G(evap)} \qquad (\text{Btu/sec})$$

where

$C_G = 1.241$ Btu/lb-°F

The rate of steam flow out of the evaporator (W_S) is determined by an implicit computation which equates the evaporator pressure with the sum of the pressure drops from the evaporator to a vacuum:

$$P_{evap} = \Delta P_{SH} + \Delta P_{piping} + \Delta P_{valve + turbine} + \Delta_{sink}$$

where

$$\Delta P_{SH} + \Delta P_{pipe} = K_6 \, (W_S)^2$$

(K_6 is such that $\Delta P_{SH} + \Delta P_{pipe} = 90$ psi for 100% W_S.)

$$\Delta P_{valve + turbine} = K_7 \frac{W_S}{\text{effective value \% } C_v}$$

(K_7 is such that $\Delta P_{valve + turbine}$ = 1255 psi for 100%; W_S and C_v = 92% of its maximum value.)

$$P_{sink} = 0 \text{ psia}$$

The heat balance equation for the evaporator water and metal is:

$$M_{evap} C_{evap} \frac{dT_{evap}}{dt} = - h_{f_g} W_S' - W_{FW} C_{FW} (T_{econ} - T_{W(evap)out})$$

where

W_S' = a net steam flow rate resulting from a difference between T_{SAT} and T_{evap}

$W_S' = K_8 (T_{evap} - T_{SAT})$, lb/sec

K_8 = a large positive number

$M_{evap} C_{evap}$ = 17,400 Btu/°F

The net rate of steam generation W_S'' is computed from:

$$W_S'' = (\text{evap power}) K_9 + W_S' \qquad \text{lb/sec}$$

where

$K_9 = 1/(h_{f_g})(T)$, as shown in Fig. A-9

The mass of saturated steam in the evaporator is computed from:

$$\rho V = \rho V_o + \int_0^t (W_S'' - W_S)\, dt \qquad \text{lb}$$

where

ρV_o = 734 lb

The evaporator pressure is computed from the density according to Fig. A-10, and the saturation temperature corresponding to this pressure is computed from the relationship shown in Fig. A-12.

3. Economizer Section

As described in Section IV-D, an iterative procedure was used to determine the circuit parameter values such that the effective capacity of the economizer was correct at 100% and 20% of full power. The transient behavior of the mean water-side temperature ($\bar{T}_{econ}$) is dominated by the water transport properties, approximated by a first-order lag with a time constant τ (14 sec at full flow), varying inversely with W_{FW}.

The economizer equations are:

$$\bar{T}_{econ} = T_{FW(in)} + \frac{1}{2} \Delta T_{W(econ)}$$

$$T_{W(econ)out} = 2\,\bar{T}_{econ} - T_{FW(in)}$$

$$\frac{1}{2} \Delta T_{W(econ)} = \frac{\Delta T_{G(econ)}\, W_G\, C_G}{2\, W_{FW}\, C_W} \left(\frac{1}{\tau_S + 1}\right)$$

where

C_W = 1.3 Btu/lb-°F

S = Laplacian argument

First Gas Lump Circuit:

$$\bar{T}_{G1} = T_{G(econ)in} - K_{10} (\bar{T}_{G1} - \bar{T}_{econ})$$

$$T_{G1(out)} = \bar{T}_{G1} - K_{10} (\bar{T}_{G1} - \bar{T}_{econ})$$

Second Gas Lump Circuit:

$$\bar{T}_{G2} = T_{G1(out)} - K_{11} (\bar{T}_{G2} - \bar{T}_{econ})$$

$$T_{G2(out)} = T_{G(out)} = \bar{T}_{G2} - K_{11} (\bar{T}_{G2} - \bar{T}_{econ})$$

K_{10} and K_{11}: see Table III

ΔU Factor Circuit:

$$\Delta U \text{ factor for } 100\% \ W_G \text{ and } W_S = 0.5 \ (50 \text{ v})$$

$$\Delta U = 52.2 - 0.155 \ W_G^{0.61} + 0.238 \ W_S^{0.8} \ (\text{volts})$$

4. Pressure Control System

The equation describing the control system was derived directly from data provided by the manufacturer of the regulator:

$$\frac{\text{fraction } C_v \text{ (max)}}{\text{psi error}} = \frac{0.77 \ (\tau_1 S + 1)}{(\tau_2 S + 1)(\tau_c S + 1)(\tau_G S + 1)(\tau_3 S + 1)}$$

where

τ_1, τ_2 = controller reset variables

τ_c = controller sensing lag = 1 sec

τ_G = governor lag = 0.4 sec

τ_3, τ_4 = controller lags = 0.3, 0.2 sec

The time constants τ_c, τ_G, τ_3, and τ_4 were found to be unimportant in all but controller set point change tests and were omitted in the tests for this report.

The dump pressure regulator was assumed to begin to open with 1280 psia upstream of turbine valve, being full open at 1330 psia (C_v linear over range). It was assumed that the throttle and dump valves had the same C_v.

Nomenclature

A	heat transfer area, ft^2
C	specific heat, Btu/lb-°F
h	heat transfer coefficient, Btu/sec-°F-ft^2
h_{f_g}	heat of vaporization of water, Btu/lb
ρ	density, lb/ft^3
M	mass, lb
P	pressure, psia
S	Laplacian argument, sec^{-1}
T	temperature, °F
U	over-all heat transfer coefficient, Btu/hr-°F-ft^2
V	volume, ft^3
W	mass flow rate, lb/sec

Subscripts

econ	economizer
evap	evaporator
FW	feedwater
G	gas side
S	steam side
SAT	saturation
(SS)	steady state
SH	superheater
turb	turbine
W	water side

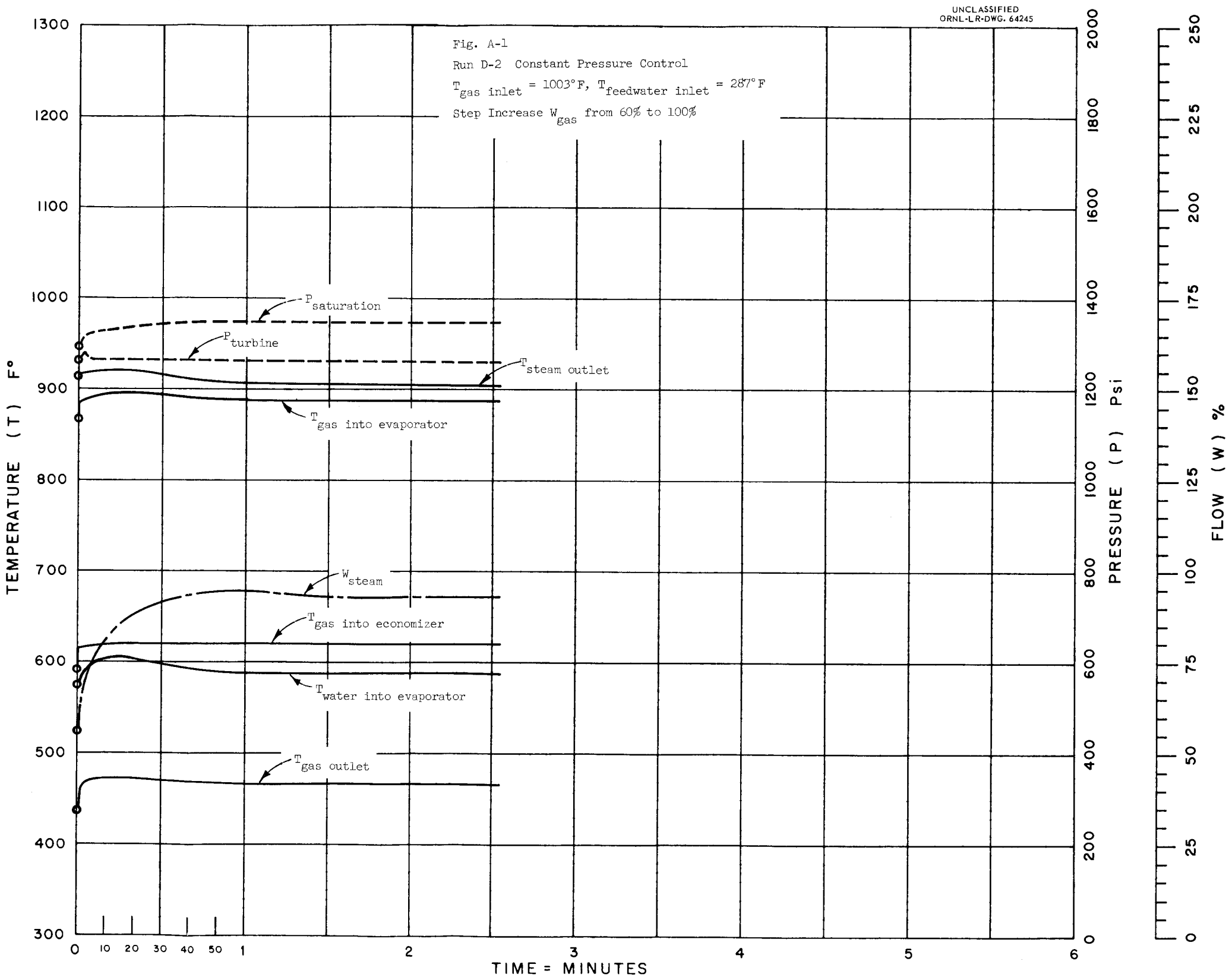
UNCLASSIFIED
ORNL-LR-DWG. 64245
Fig. A-1
Run D-2 Constant Pressure Control
$T_{gas\ inlet}$ = 1003°F, $T_{feedwater\ inlet}$ = 287°F
Step Increase W_{gas} from 60% to 100%
$P_{saturation}$
$P_{turbine}$
$T_{steam\ outlet}$
$T_{gas\ into\ evaporator}$
W_{steam}
$T_{gas\ into\ economizer}$
$T_{water\ into\ evaporator}$
$T_{gas\ outlet}$
TEMPERATURE (T) F°
PRESSURE (P) Psi
FLOW (W) %
TIME = MINUTES
1300
1200
1100
1000
900
800
700
600
500
400
300
2000
1800
1600
1400
1200
1000
800
600
400
200
0
250
225
200
175
150
125
100
75
50
25
0
0
10
20
30
40
50
1
2
3
4
5
6

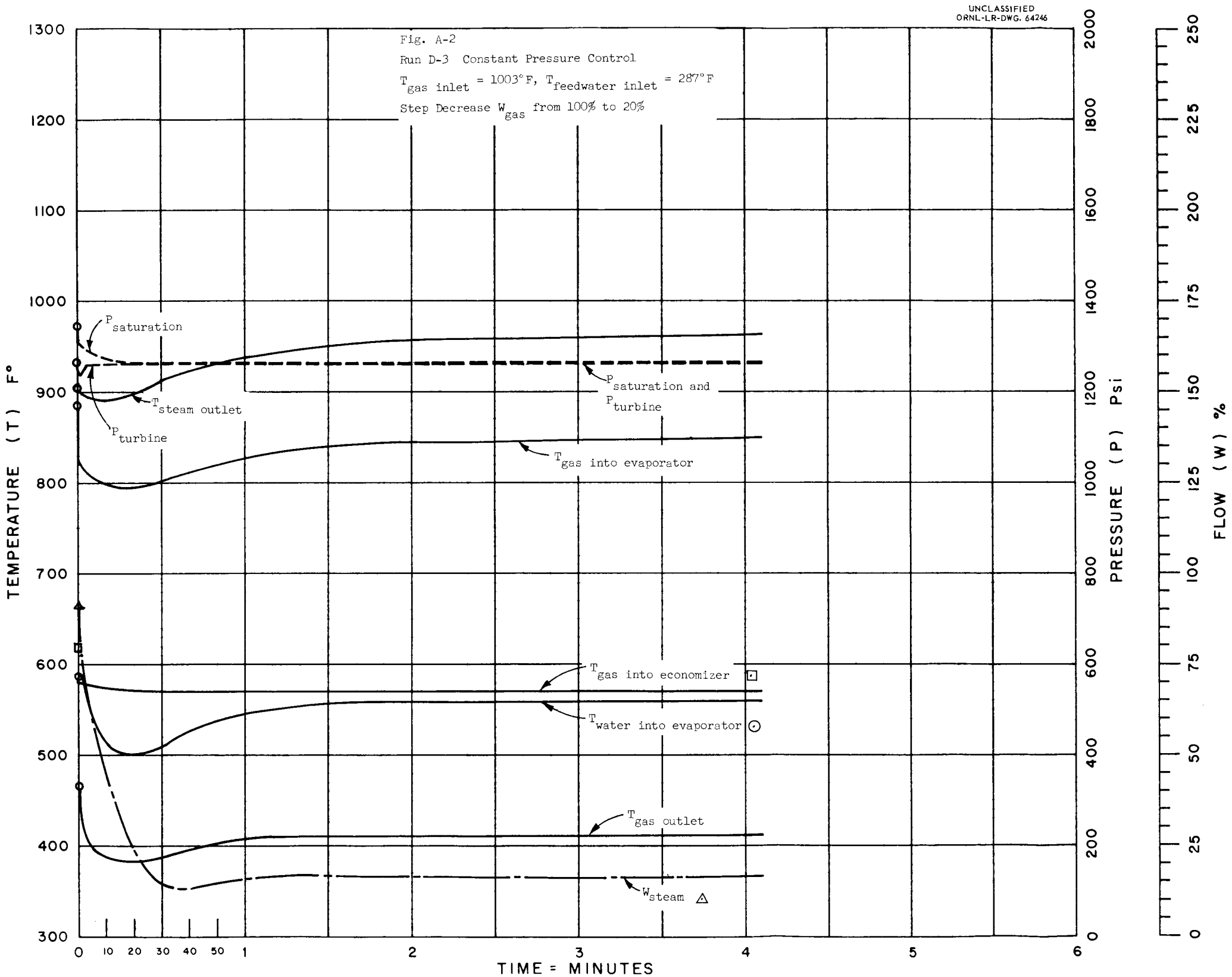
UNCLASSIFIED
ORNL-LR-DWG. 64246
Fig. A-2
Run D-3 Constant Pressure Control
$T_{gas\ inlet}$ = 1003°F, $T_{feedwater\ inlet}$ = 287°F
Step Decrease W_{gas} from 100% to 20%
$P_{saturation}$
$T_{steam\ outlet}$
$P_{turbine}$
$P_{saturation}$ and $P_{turbine}$
$T_{gas\ into\ evaporator}$
$T_{gas\ into\ economizer}$
$T_{water\ into\ evaporator}$
$T_{gas\ outlet}$
W_{steam}
TEMPERATURE (T) F°
PRESSURE (P) Psi
FLOW (W) %
TIME = MINUTES
1300
1200
1100
1000
900
800
700
600
500
400
300
2000
1800
1600
1400
1200
1000
800
600
400
200
0
250
225
200
175
150
125
100
75
50
25
0
0
10
20
30
40
50
1
2
3
4
5
6

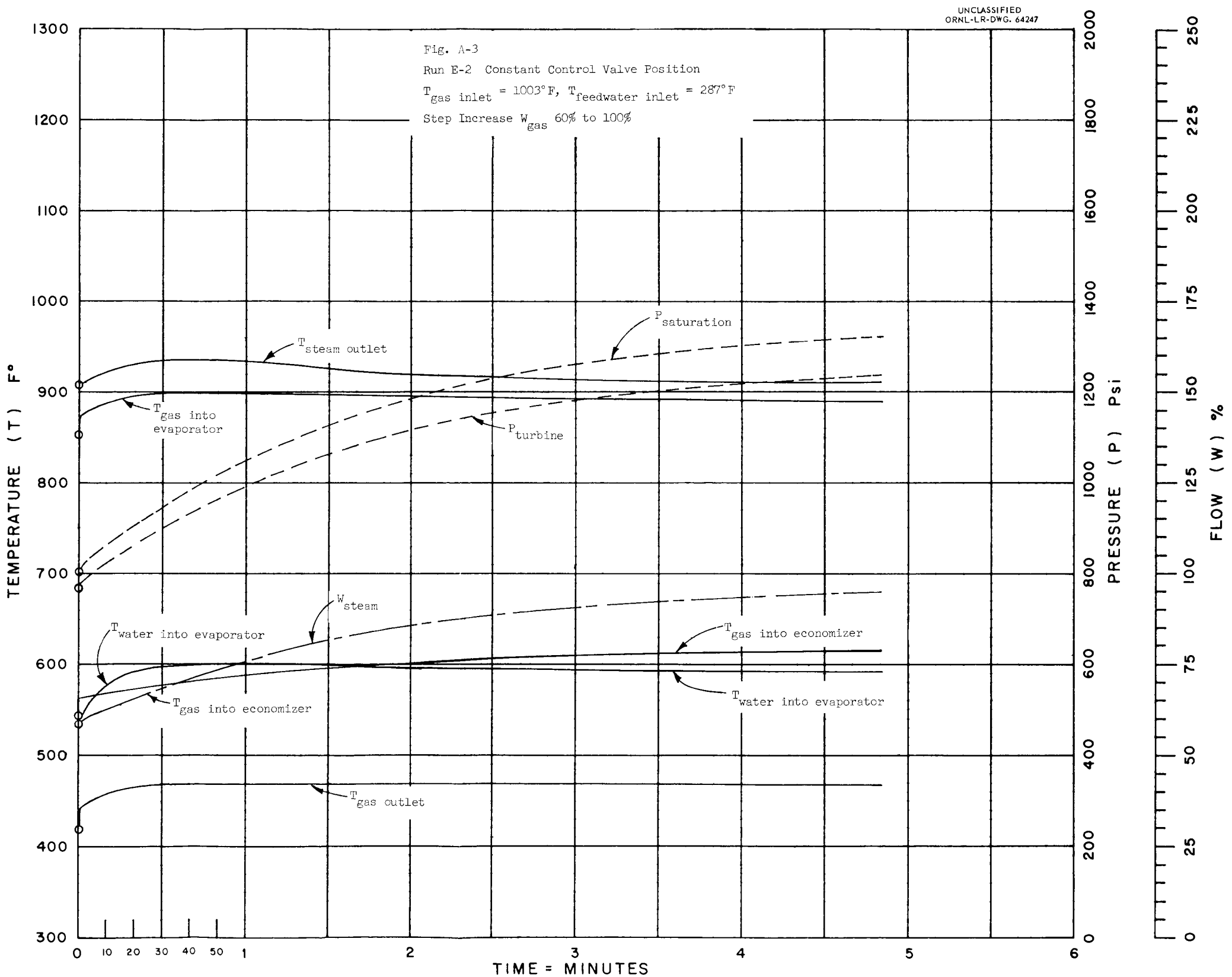
UNCLASSIFIED
ORNL-LR-DWG. 64247
Fig. A-3
Run E-2 Constant Control Valve Position
$T_{gas\ inlet}$ = 1003°F, $T_{feedwater\ inlet}$ = 287°F
Step Increase W_{gas} 60% to 100%
$P_{saturation}$
$T_{steam\ outlet}$
$T_{gas\ into\ evaporator}$
$P_{turbine}$
W_{steam}
$T_{water\ into\ evaporator}$
$T_{gas\ into\ economizer}$
$T_{gas\ into\ economizer}$
$T_{water\ into\ evaporator}$
$T_{gas\ outlet}$
TEMPERATURE (T) F°
PRESSURE (P) Psi
FLOW (W) %
TIME = MINUTES
1300
1200
1100
1000
900
800
700
600
500
400
300
2000
1800
1600
1400
1200
1000
800
600
400
200
0
250
225
200
175
150
125
100
75
50
25
0
0
10
20
30
40
50
1
2
3
4
5
6

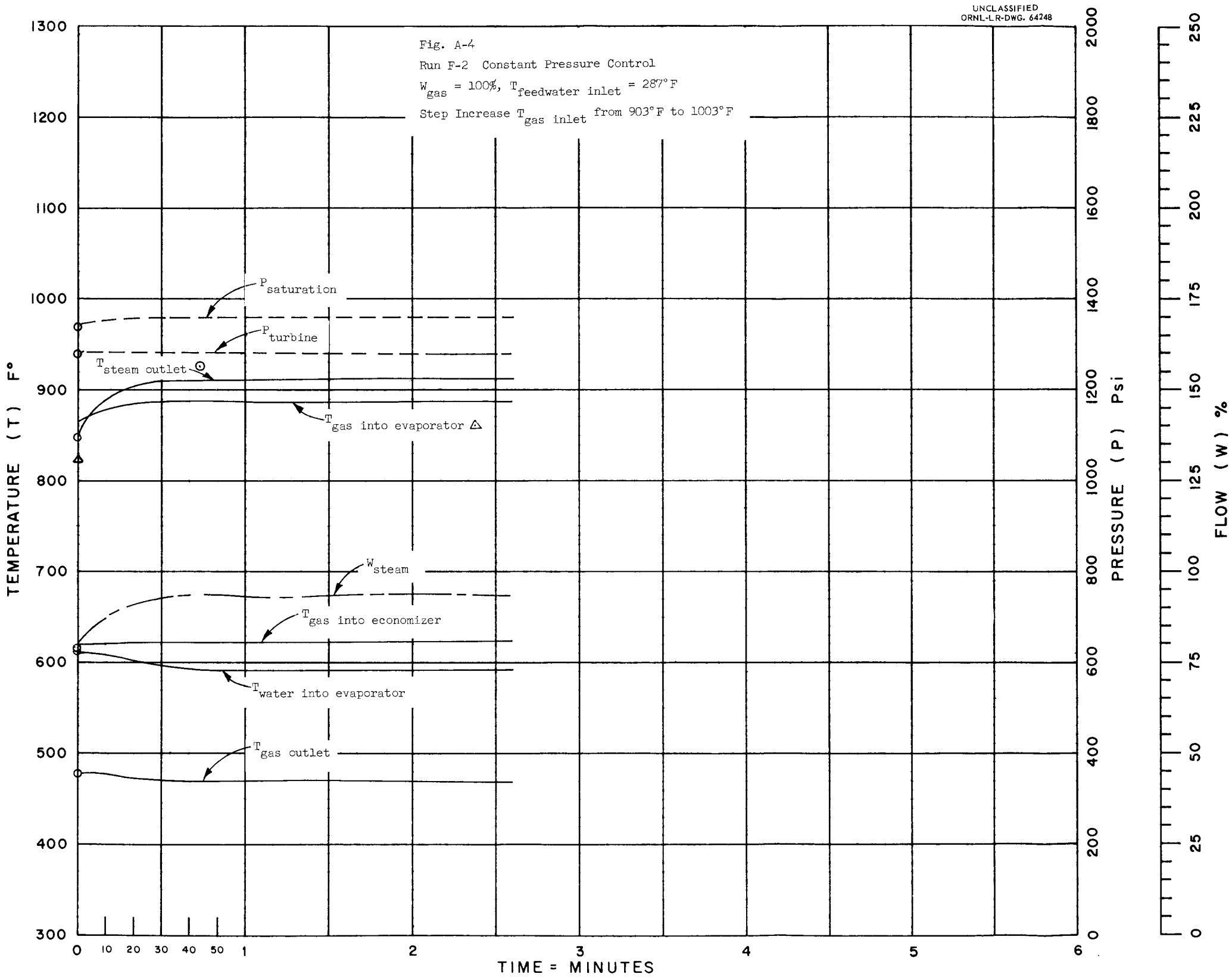
UNCLASSIFIED
ORNL-LR-DWG. 64248
Fig. A-4
Run F-2 Constant Pressure Control
W_{gas} = 100%, $T_{feedwater\ inlet}$ = 287°F
Step Increase $T_{gas\ inlet}$ from 903°F to 1003°F
$P_{saturation}$
$P_{turbine}$
$T_{steam\ outlet}$
$T_{gas\ into\ evaporator}$
W_{steam}
$T_{gas\ into\ economizer}$
$T_{water\ into\ evaporator}$
$T_{gas\ outlet}$
TEMPERATURE (T) F°
PRESSURE (P) Psi
FLOW (W) %
TIME = MINUTES
1300
1200
1100
1000
900
800
700
600
500
400
300
2000
1800
1600
1400
1200
1000
800
600
400
200
0
250
225
200
175
150
125
100
75
50
25
0
0
10
20
30
40
50
1
2
3
4
5
6

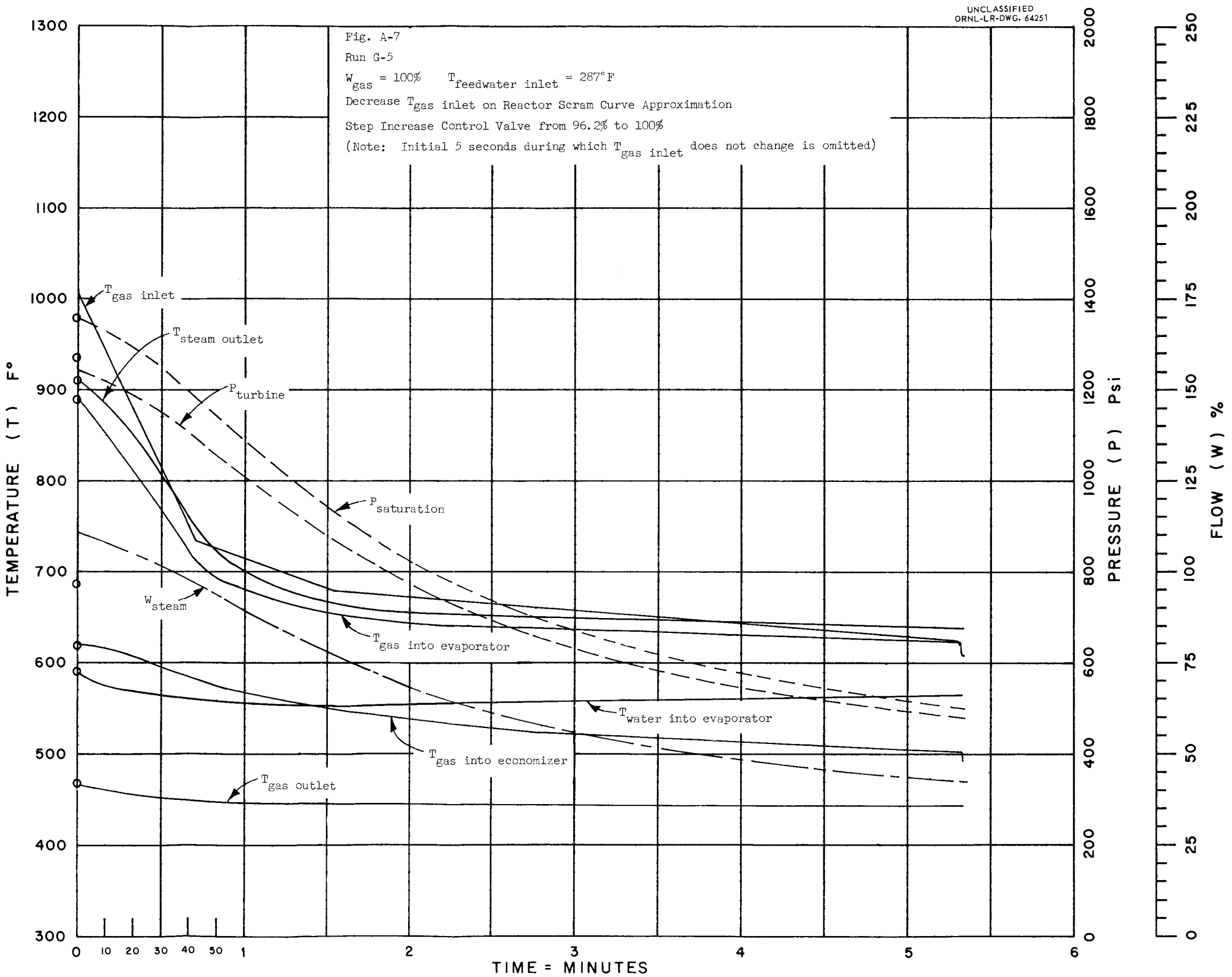
UNCLASSIFIED
ORNL-LR-DWG. 64251
Fig. A-7
Run G-5
W_{gas} = 100% $T_{feedwater\ inlet}$ = 287°F
Decrease $T_{gas\ inlet}$ on Reactor Scram Curve Approximation
Step Increase Control Valve from 96.2% to 100%
(Note: Initial 5 seconds during which $T_{gas\ inlet}$ does not change is omitted)
$T_{gas\ inlet}$
$T_{steam\ outlet}$
$P_{turbine}$
$P_{saturation}$
W_{steam}
$T_{gas\ into\ evaporator}$
$T_{water\ into\ evaporator}$
$T_{gas\ into\ economizer}$
$T_{gas\ outlet}$
TEMPERATURE (T) F°
PRESSURE (P) Psi
FLOW (W) %
TIME = MINUTES
1300
1200
1100
1000
900
800
700
600
500
400
300
2000
1800
1600
1400
1200
1000
800
600
400
200
0
250
225
200
175
150
125
100
75
50
25
0
0
10
20
30
40
50
1
2
3
4
5
6

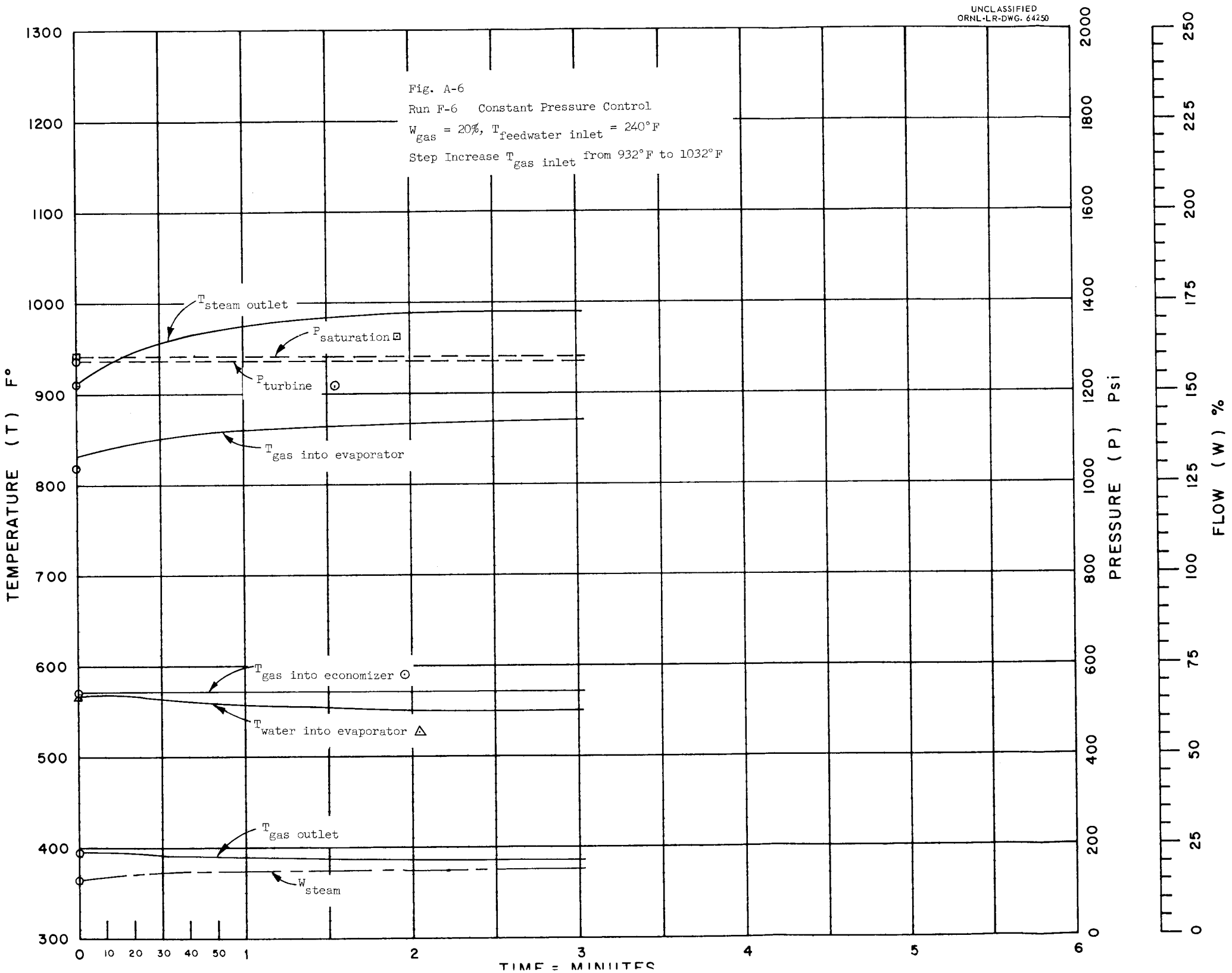
UNCLASSIFIED
ORNL-LR-DWG. 64250
Fig. A-6
Run F-6 Constant Pressure Control
W_{gas} = 20%, $T_{feedwater\ inlet}$ = 240°F
Step Increase $T_{gas\ inlet}$ from 932°F to 1032°F
$T_{steam\ outlet}$
$P_{saturation}$
$P_{turbine}$
$T_{gas\ into\ evaporator}$
$T_{gas\ into\ economizer}$
$T_{water\ into\ evaporator}$
$T_{gas\ outlet}$
W_{steam}
TEMPERATURE (T) F°
PRESSURE (P) Psi
FLOW (W) %
TIME = MINUTES
1300
1200
1100
1000
900
800
700
600
500
400
300
2000
1800
1600
1400
1200
1000
800
600
400
200
0
250
225
200
175
150
125
100
75
50
25
0
0
10
20
30
40
50
1
2
3
4
5
6

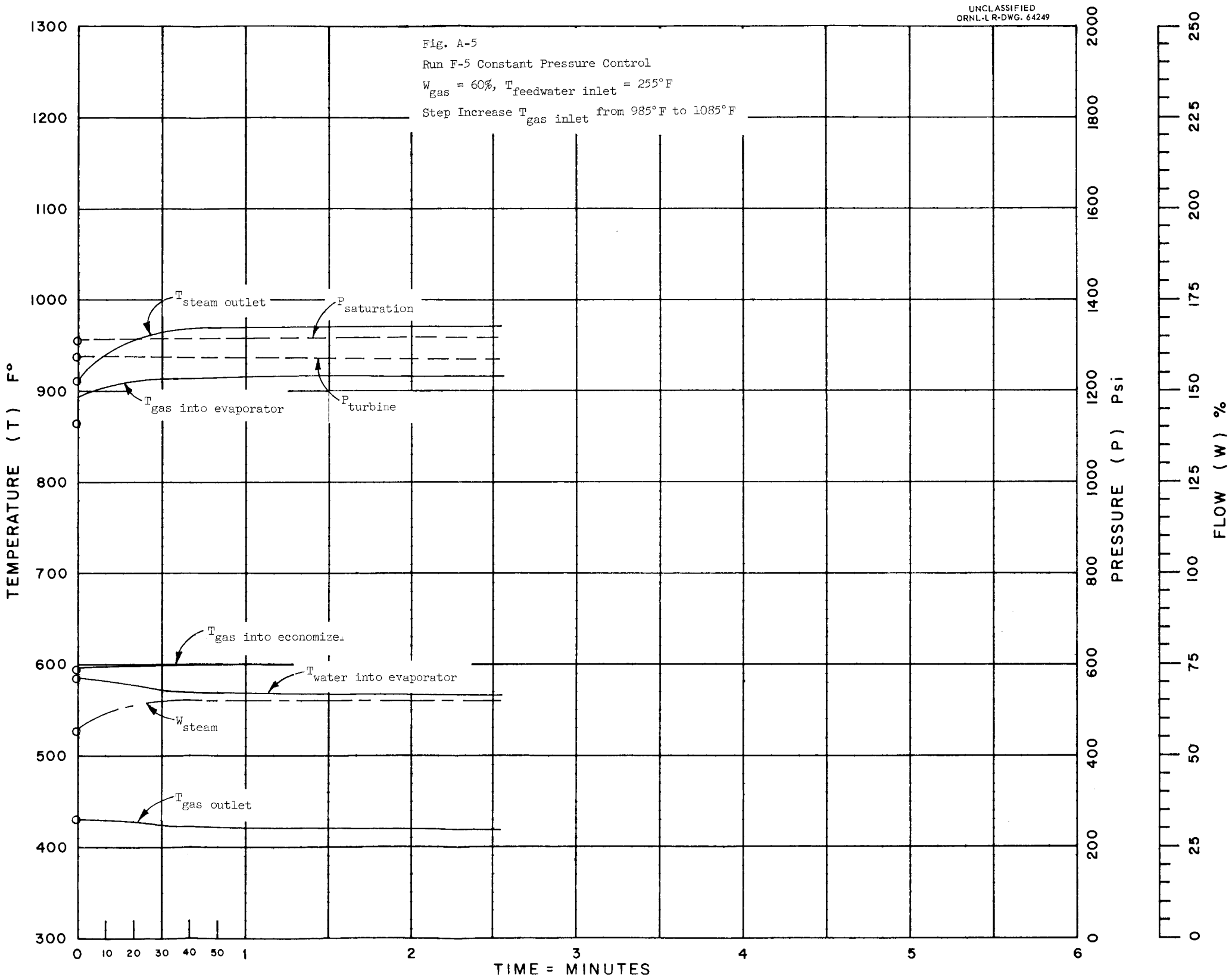
UNCLASSIFIED
ORNL-LR-DWG. 64249
Fig. A-5
Run F-5 Constant Pressure Control
W_{gas} = 60%, $T_{feedwater\ inlet}$ = 255°F
Step Increase $T_{gas\ inlet}$ from 985°F to 1085°F
$T_{steam\ outlet}$
$P_{saturation}$
$T_{gas\ into\ evaporator}$
$P_{turbine}$
$T_{gas\ into\ economizer}$
$T_{water\ into\ evaporator}$
W_{steam}
$T_{gas\ outlet}$
TEMPERATURE (T) F°
PRESSURE (P) Psi
FLOW (W) %
TIME = MINUTES
1300
1200
1100
1000
900
800
700
600
500
400
300
2000
1800
1600
1400
1200
1000
800
600
400
200
0
250
225
200
175
150
125
100
75
50
25
0
0
10
20
30
40
50
1
2
3
4
5
6

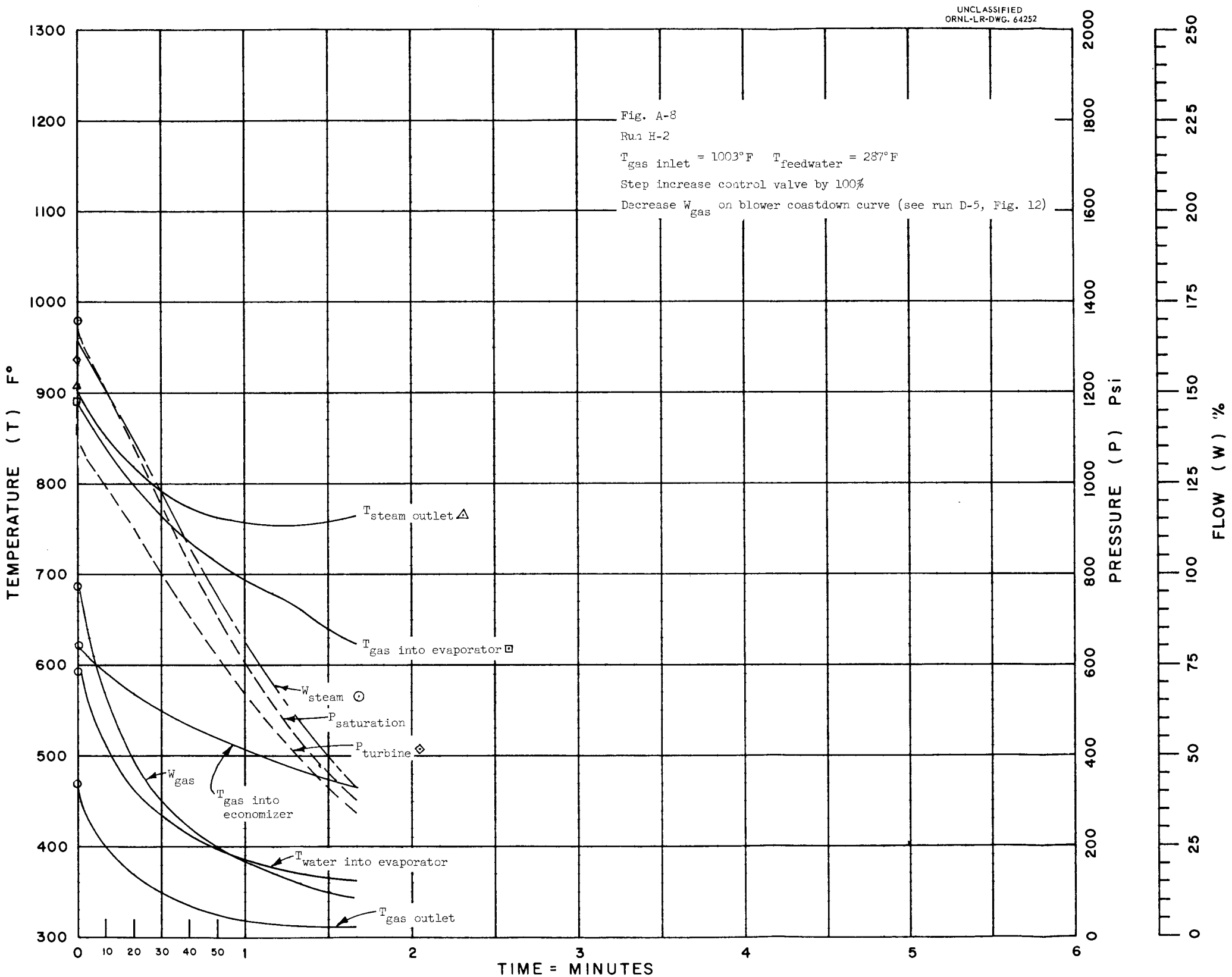
UNCLASSIFIED
ORNL-LR-DWG. 64252
Fig. A-8
Run H-2
$T_{gas\ inlet}$ = 1003°F $T_{feedwater}$ = 287°F
Step increase control valve by 100%
Decrease W_{gas} on blower coastdown curve (see run D-5, Fig. 12)
$T_{steam\ outlet}$
$T_{gas\ into\ evaporator}$
W_{steam}
$P_{saturation}$
$P_{turbine}$
W_{gas}
$T_{gas\ into\ economizer}$
$T_{water\ into\ evaporator}$
$T_{gas\ outlet}$
TEMPERATURE (T) F°
PRESSURE (P) Psi
FLOW (W) %
TIME = MINUTES
1300
1200
1100
1000
900
800
700
600
500
400
300
2000
1800
1600
1400
1200
1000
800
600
400
200
0
250
225
200
175
150
125
100
75
50
25
0
0
10
20
30
40
50
1
2
3
4
5
6

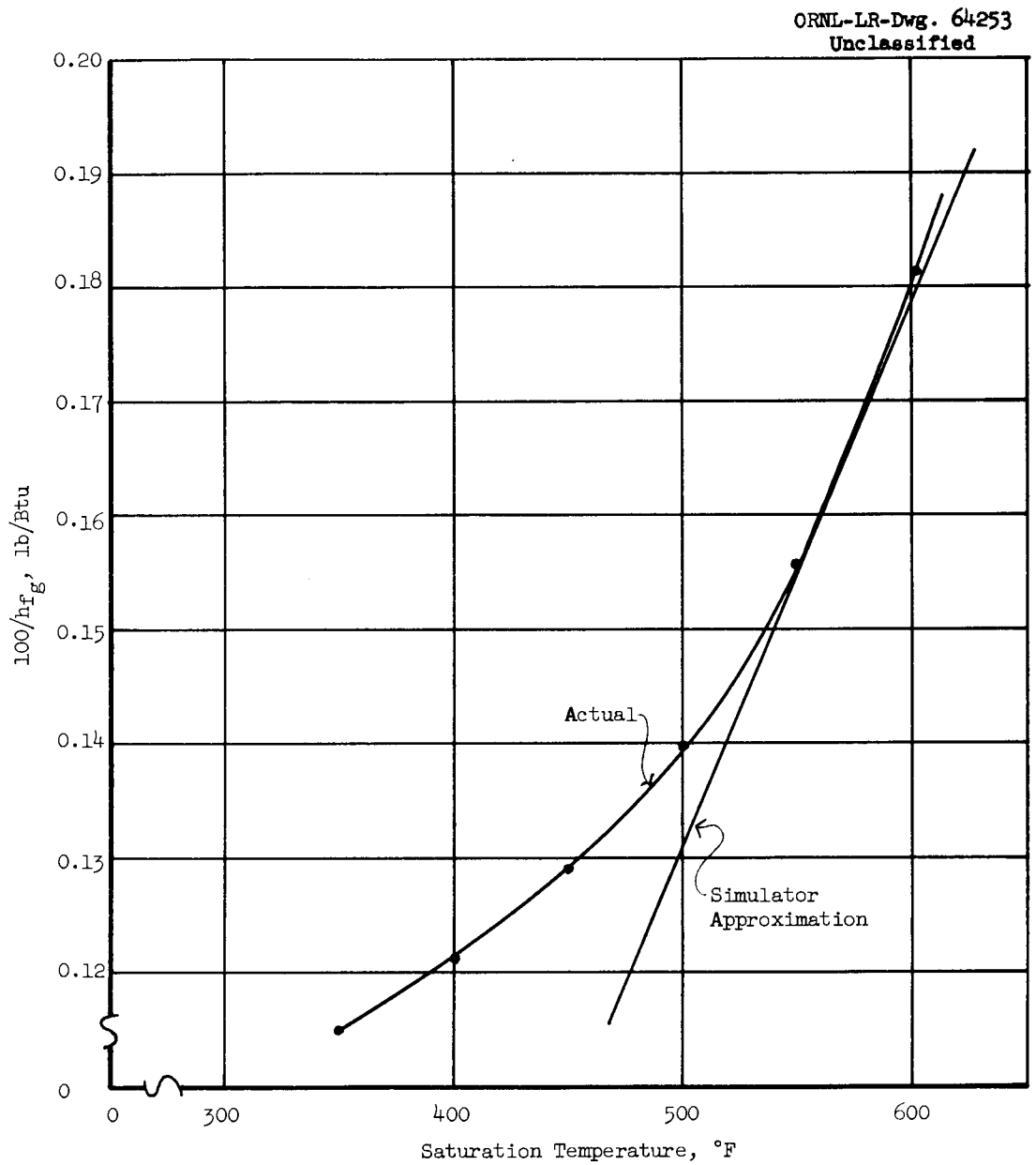

Fig. A-9. Reciprocal Heat of Vaporization (h_{fg}) vs Saturation Temperature

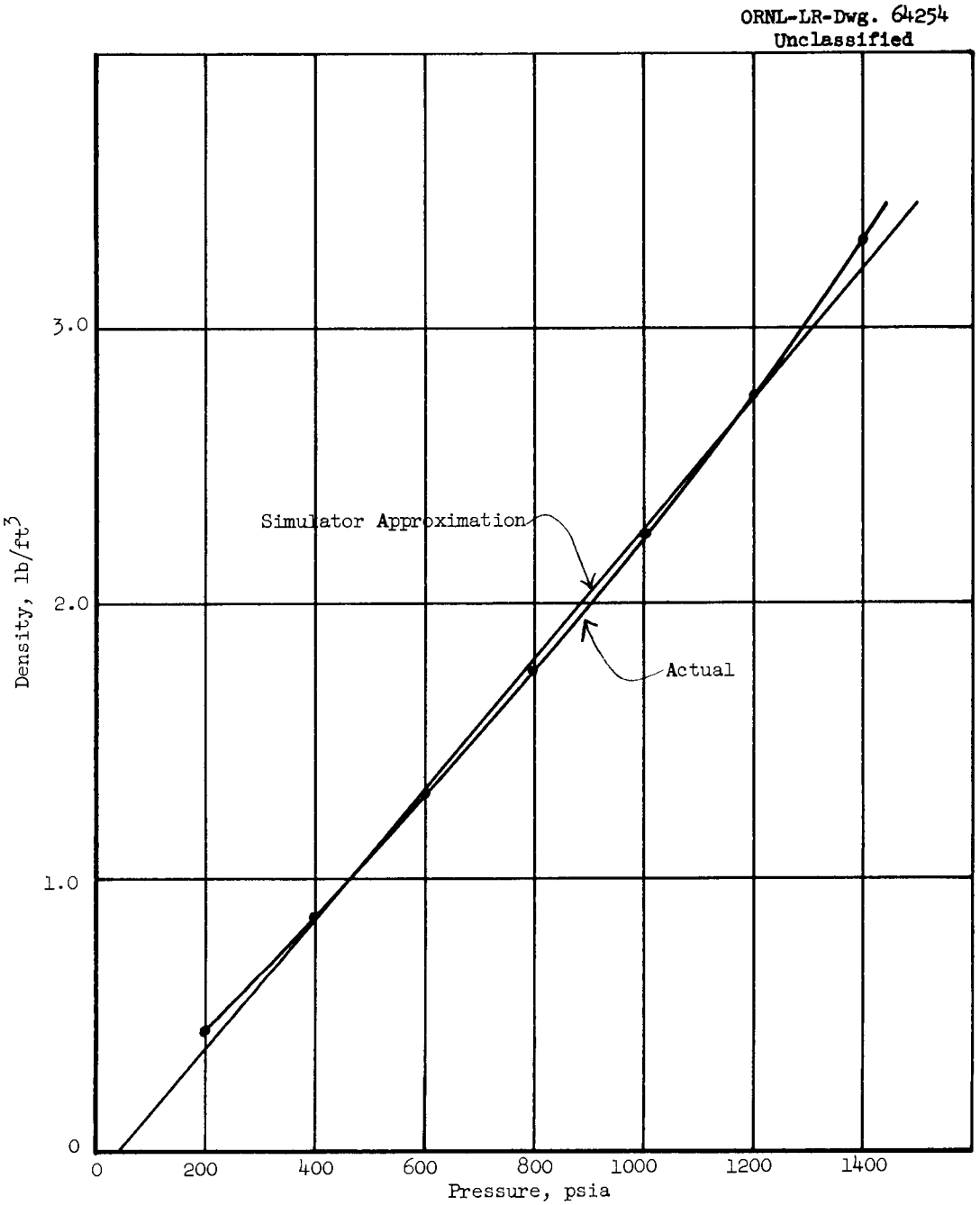

Fig. A-10. Saturation Density vs Pressure for H_2O

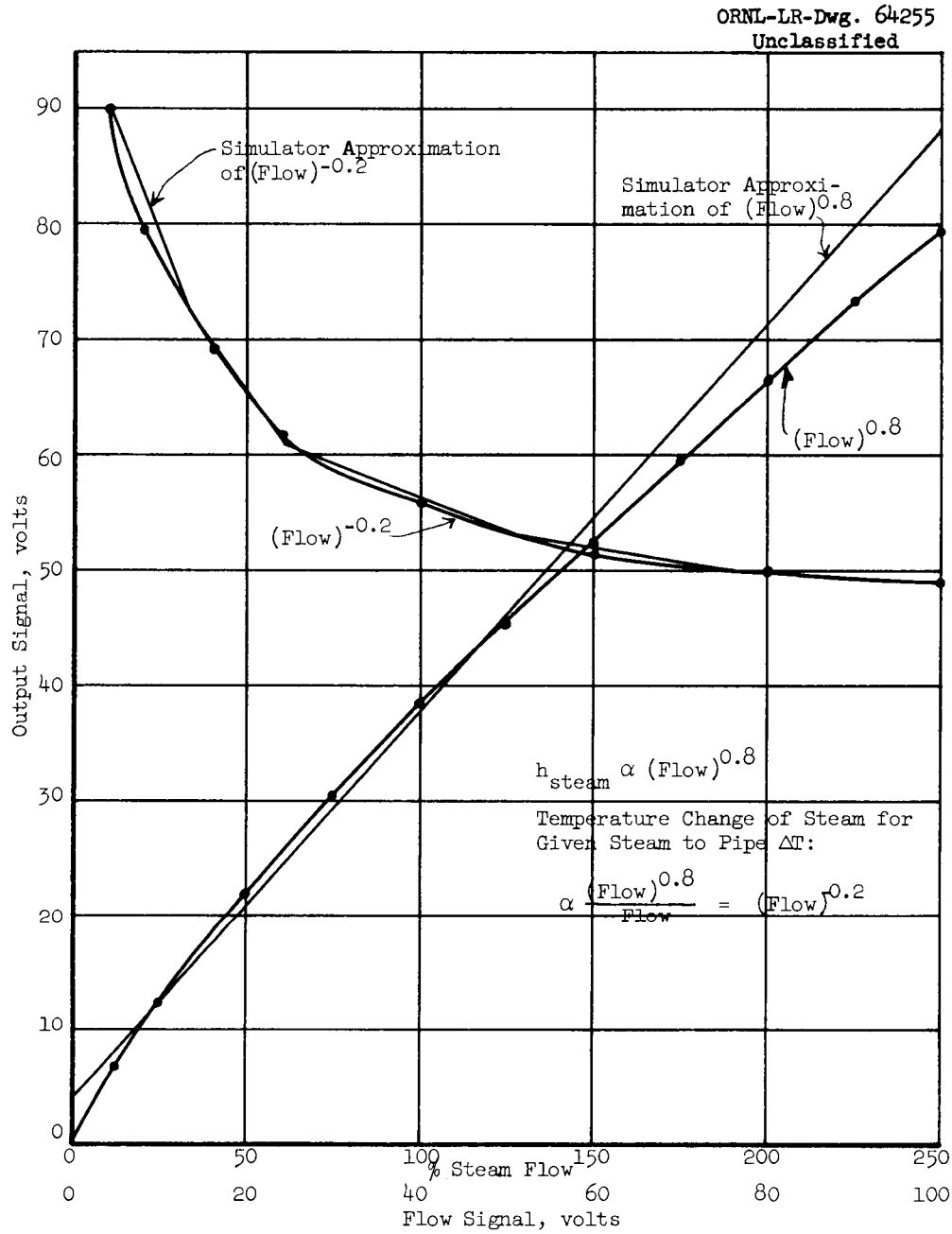

Fig. A-11. Steam Heat Transfer Properties as Functions of Steam Flow Rate

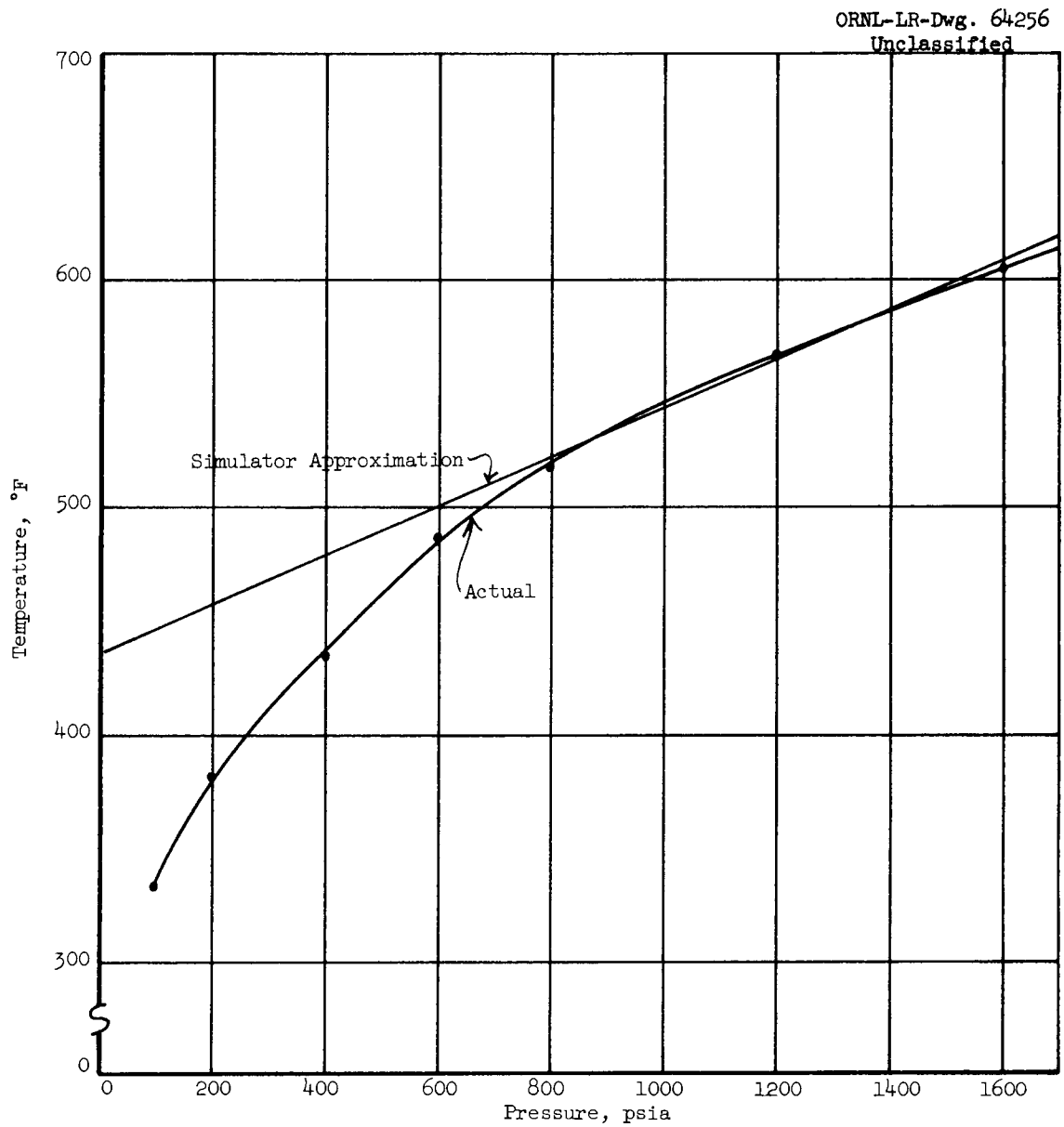

Fig. A-12. Saturation Temperature vs Pressure for H_2O

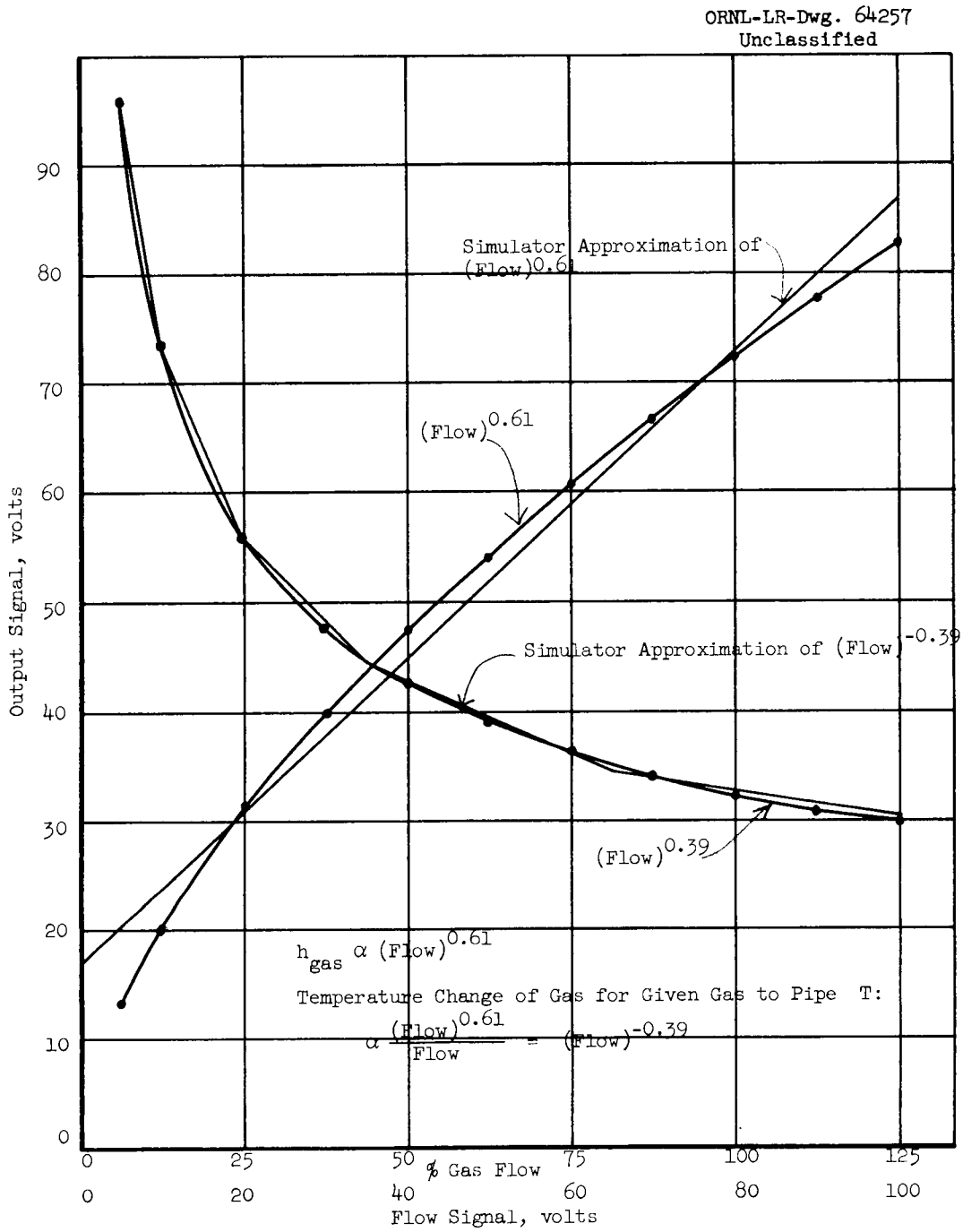

Fig. A-13. Gas Heat Transfer Properties as Functions of Gas Flow Rate

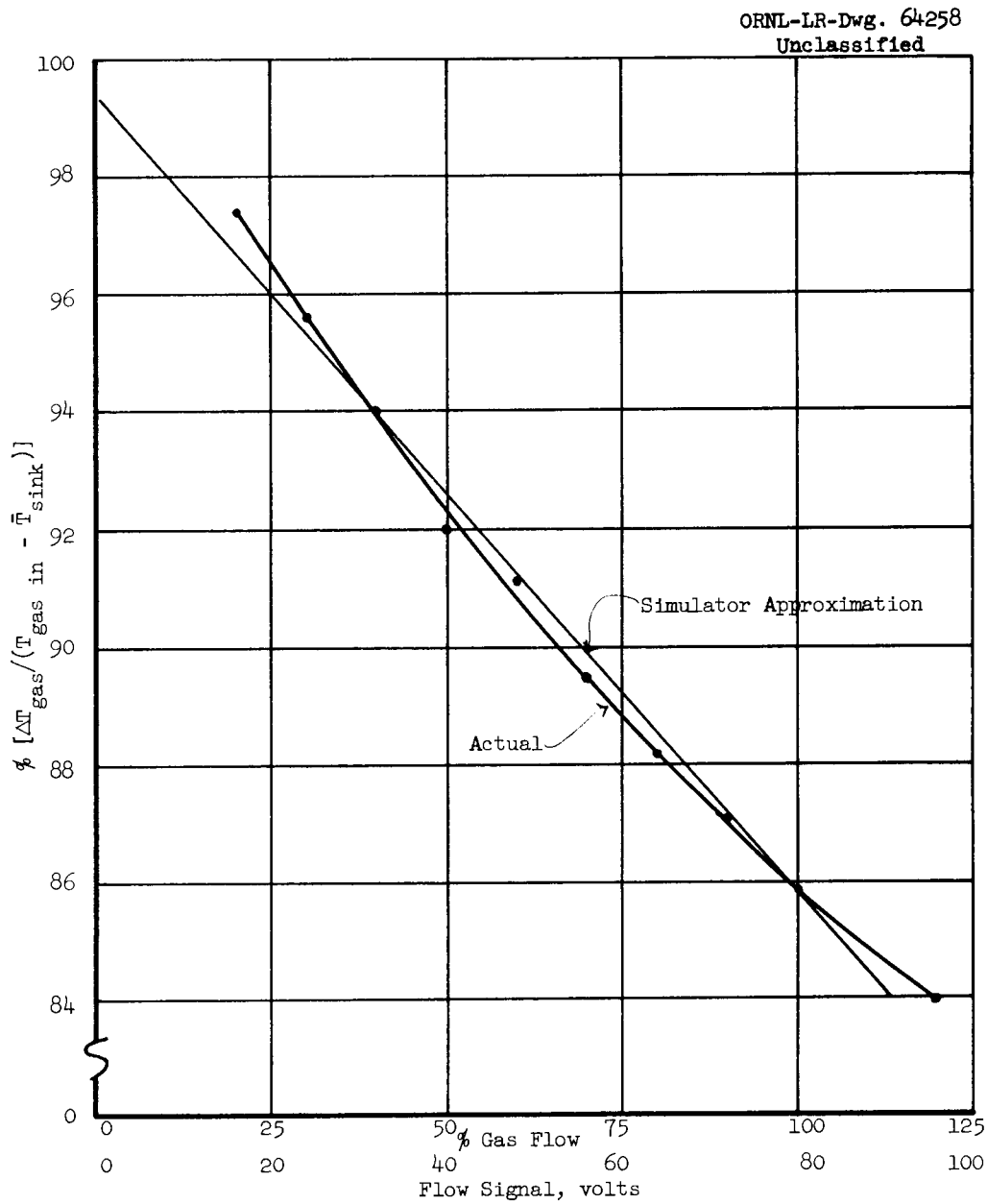

Fig. A-14. Per Cent Change in Gas Temperature Through Evaporator vs Gas Flow

UNCLASSIFIED
ORNL-LR-DWG. 63943

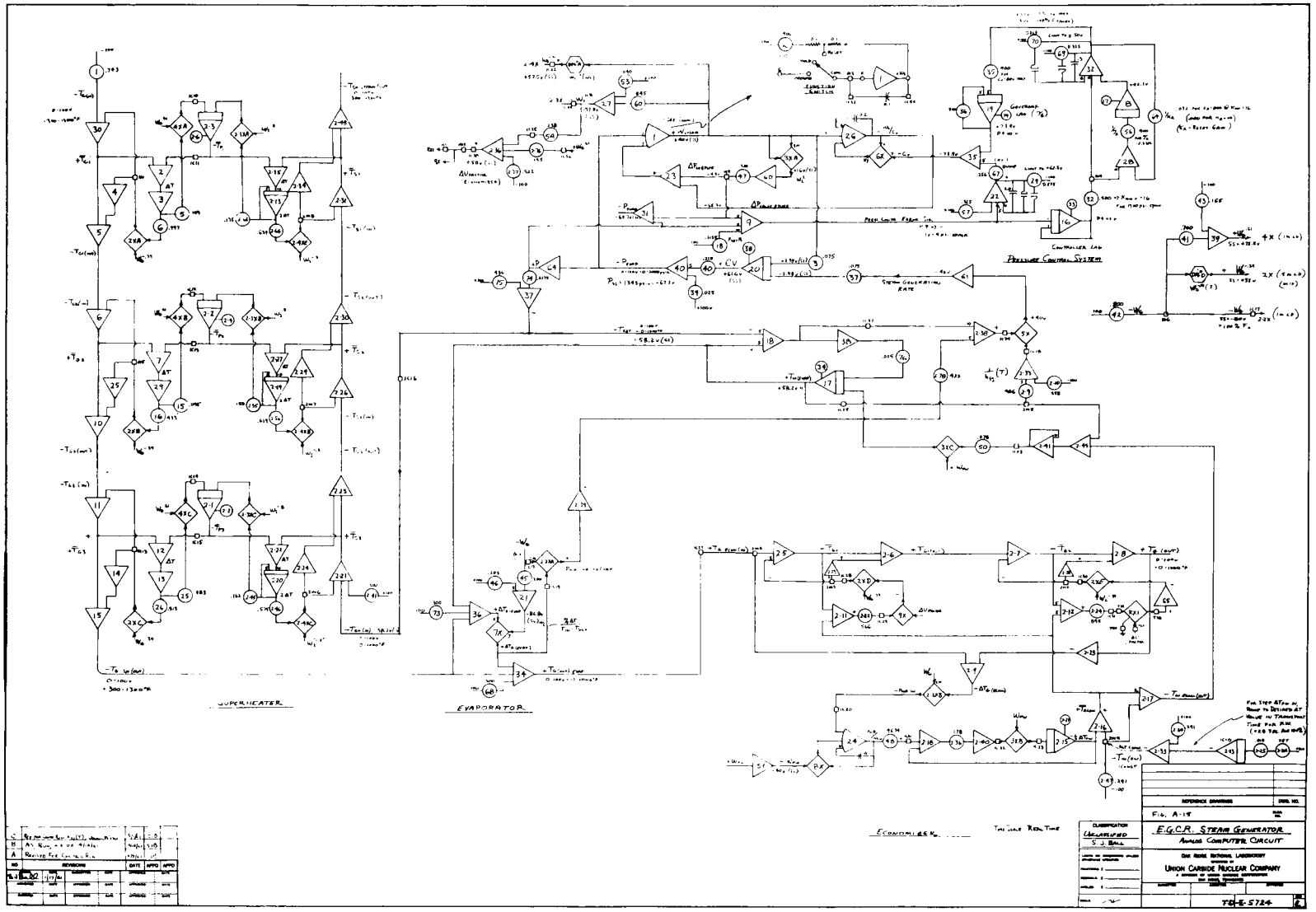

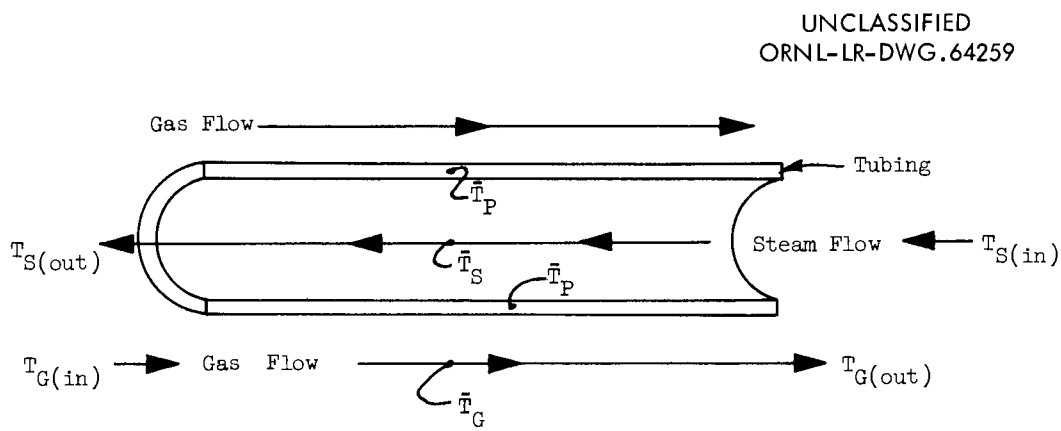

Fig. A-16. Typical Section of Superheater

References

1) R. A. Bourman, A. C. Mueller, and W. M. Nagle, Trans. ASME, May 1940, p 283-294.

2) W. H. McAdams, Heat Transmission, 3rd ed., p 272, McGraw-Hill, New York, 1954.

3) W. H. McAdams, W. E. Kennel, and J. N. Addoms, Trans. ASME, 72, 1950, p 421-428.

4) K. A. Gardiner, Efficiency of Extended Surface, Trans. ASME, November 1945, p 621.

5) D. L. Katz, et al., Correlation of Heat Transfer and Pressure Drop for Air Flowing Across Banks of Finned Tubes, Rep. No. 30, Engineering Research Institute, University of Michigan, December 1954.

6) W. M. Kays and A. L. London, Compact Heat Exchangers, National Press, 1955.

7) G. C. Robinson and M. M. Yarosh, Trip Report to C. F. Braun Company, August 1, 1961.

8) A. E. Rogers and T. W. Connolly, Analog Computation in Engineering Design, McGraw-Hill, 1960, p 194-6.

9) D. B. Hinton, Thermal Characteristics of Fluid Flow in Pipes, ORNL CF-60-9-116, September 13, 1960.

Internal Distribution

1. R. K. Adams
2-4. S. J. Ball
5. S. E. Beall
6-8. M. Bender
9. A. L. Boch
10. C. J. Borkowski
11. R. B. Briggs
12. O. W. Burke
13. J. H. Coobs
14. W. B. Cottrell
15. J. H. DeVan
16. D. A. Douglas
17. M. H. Fontana
18. J. Foster
19. A. P. Fraas
20. B. L. Greenstreet
21. L. A. Haack
22. W. O. Harms
23. C. S. Harrill
24. P. G. Herndon
25. H. W. Hoffman
26. O. H. Klepper
27. R. B. Korsmeyer
28. C. E. Larson (K-25)
29. R. N. Lyon
30. H. G. MacPherson
31-49. W. D. Manly
50-52. E. R. Mann
53. A. J. Miller
54. R. L. Moore
55. F. H. Neill
56. A. M. Perry
57. C. A. Preskitt
58. M. W. Rosenthal
59. G. Samuels
60. H. W. Savage
61. A. W. Savolainen
62. O. Sisman
63. M. J. Skinner
64. I. Spiewak
65. R. S. Stone
66. E. Storto
67. J. A. Swartout
68. D. B. Trauger
69. C. S. Walker
70. G. M. Watson
71-72. G. D. Whitman
73. C. E. Winters
74-85. M. M. Yarosh
86-88. Laboratory Records Department
89. Laboratory Records Department, R.C.
90-91. Central Research Library
92-94. Y-12 Technical Library
Document Reference Section

External Distribution

95-96. W. R. Cooper, TVA
97-106. L. H. Jackson, AEC, ORO
107. A. W. Meagher, TVA
108-122. Division of Technical Information Extension
123. Research and Development Division, AEC, ORO
124-125. Reactor Division, AEC, ORO